PARVALBUMIN INTERNEURON VULNERABILITY IN NERVOUS SYSTEM INJURY AND DISEASE

By

Jacob Benjamin Ruden

Dissertation

Submitted to the Faculty of the

Graduate School of Vanderbilt University

in partial fulfillment of the requirements

for the degree of

DOCTOR OF PHILOSOPHY

in

Neuroscience

May 13, 2022

Nashville, Tennessee

Approved:

Christine Konradi, Ph.D.

Eric Delpire, Ph.D.

Laura L. Dugan, M.D.

Brad Grueter, Ph.D.

To Sarah and my parents, for always believing in me

ACKNOWLEDGMENTS

The work described in this dissertation was supported by MH064913, AG033679, AG058856, TR002243, GM07628, VA Tennessee Valley Geriatric Research, Education and Clinical Center (GRECC), Vanderbilt Institute for Clinical and Translational Research, and the Abram C. Shmerling Professorship. I would like to acknowledge my co-authors on the forthcoming hypoxia manuscript: Oscar Diaz-Ruiz, Savitri Chakraborty, Mikiyas Daniel, Mrinalini Dixit, Jeanette Saskowski, and Laura L. Dugan. Thank you to Taylor Sherrill, Harikrishna Tanjore, and Timothy Blackwell for generous access to their hypoxia chamber, and for advice about optimizing the protocol. Thank you to Aaron Bowman for sharing the CC3 iPSC line.

Classroom and personal experience inspired me to pursue a PhD in Neuroscience. Seminar courses exposed the disconnect between scientific discoveries and treatment options for neurodegenerative and psychiatric diseases, and I witnessed my grandmother struggle to be a caregiver when my step-grandfather was diagnosed with Alzheimer's disease.

I would like to thank my advisor, Laura Dugan, for her constant support throughout the years. Laura has supported my pursuits both within and outside of the laboratory, including regarding my choice to pursue a career in science policy. Even when experiments failed, she always helped me to see the potential for something positive and worthwhile to learn from them. Thank you to my committee members, Eric Delpire, Brad Grueter, and Christine Konradi, for providing invaluable guidance regarding next steps for my project. Special thanks to Christine for meeting with me twice a month for much of my time at Vanderbilt. Christine helped me troubleshoot experiments and wrote a review article with me, but what I will miss the most are our conversations about the state of our world and the state of science.

Thank you to all the past and present members of the Dugan Laboratory for making the laboratory feel like my second home in Nashville. Special thanks to Neena Dixit for ensuring that an upcoming celebration of some sort was always on the calendar (including masked and socially distanced celebrations during the pandemic), and to Jeanette Saskowski for keeping the laboratory well-stocked and always running smoothly. Pre-pandemic, I had lunch daily with Neena and Jeanette, and I have truly missed our conversations these last couple of years. I also want to thank the administrative staff who work tirelessly behind the scenes to make our lives easier, including Terri Ray, Roz Johnson, Beth Sims, Pammy Doss, and Darlene Pope.

I want to thank all my "new" friends that I have met since moving to Nashville for making my time here a lot of fun and reminding me about the importance of life outside of the laboratory. You all are making it very difficult to leave this town! Thank you to all my "old" friends for being better than I have been about staying in touch long-distance and for being genuinely interested in what I've been doing in the laboratory.

I am thankful to my family members (including all the family that I "gained" on June 1, 2019!) for their guidance and support. I'm grateful that my sister-in-law Julia chose to move to Nashville for her job. We've loved spending countless Shabbat dinners, road trips, and other adventures with you since you moved here. Thank you to my parents for being constant sources of love and support. You both have been willing to listen to me countless times when I've called to complain about a failed experiment or anything else.

My last thank you is reserved for my rock and the love of my life, Sarah Paige. This dissertation belongs to you as much as it belongs to me, as I can't imagine a world in which I would have gone through graduate school without you by my side. Te amo/אני אוהב אותך/I love you.

TABLE OF CONTENTS

Page

LIST OF TABLES

LIST OF FIGURES

CHAPTER 1

Introduction

1.1 Background

Approximately 6.5 million people in the United States are currently living with Alzheimer's disease [1]. Since older age is the greatest risk factor for Alzheimer's disease and the large post-World War II generation is becoming older, projections suggest that this number will more than double by 2060 [1, 2]. Alzheimer's disease and other neurodegenerative diseases are associated with both financial and personal burdens, and there are currently no known treatments that can prevent these diseases or slow their progression [3]. Treatments for schizophrenia and other psychiatric diseases are limited and often result in severe side effects [4]. Understanding fundamental mechanisms which underlie Alzheimer's disease, schizophrenia, and other devastating brain disorders is imperative to begin to design treatments to prevent or delay these disorders. This is what led to my choice of dissertation topic.

1.2 Parvalbumin Interneuron Vulnerability

Selective injury to specific subpopulations of interneurons may be important to many brain disorders. This dissertation focuses on one subpopulation of inhibitory GABAergic interneurons, parvalbumin-expressing interneurons (PV-INs), which have been proposed as selectively vulnerable to injury across a broad range of nervous system disorders [5, 6]. PV-INs are defined by the presence of the calcium-binding protein parvalbumin and by their fast-spiking phenotype [5]. They are found in low abundance throughout neocortex,

hippocampus, and basal forebrain [5, 7]. PV-INs express both GAD65 and GAD67, and their dendrites are largely aspiny [5, 8, 9]. PV-IN-related changes have been observed in many diseases and disorders, including in Alzheimer's disease, schizophrenia, and autism spectrum disorder [10-16]. Chapter 2 of this dissertation explains in detail what PV-INs are, discusses how PV-INs are vulnerable, and presents some potential explanations for why they may be so vulnerable.

1.3 *Pvalb* and Parvalbumin

The *Pvalb* gene is regulated by epigenetic mechanisms. Histone deacetylases repress *Pvalb* gene transcription during development via histone deacetylase 1 binding at the *Pvalb* promoter, resulting in less expression of parvalbumin [17]. Exposure to maternal manganese resulted in *Pvalb* promoter hypermethylation [18]. Increased *Pvalb* promoter hypermethylation was found in postmortem hippocampus from individuals with schizophrenia [19]. Additionally, administration of phencyclidine, an addictive drug of abuse, resulted in *Pvalb* promoter hypermethylation in rat prefrontal cortex and hippocampus [20]. Increased *Pvalb* promoter methylation was also found in individuals dependent on methamphetamine, another addictive drug of abuse [21]. Methylation leads to less expression of *Pvalb*, which in turn results in less expression of parvalbumin [18, 21]. Reduced parvalbumin protein expression is likely detrimental to PV-INs, as discussed in detail in Chapter 5. Parvalbumin, an EF-hand protein with a helix–loop–helix motif, is not known to have any binding partners [22]. Two of the three EF-hand domains can bind calcium and magnesium [22]. Older literature suggests that the half-life of parvalbumin in rat dorsal root ganglion neurons is about 6 minutes [23].

1.4 Parvalbumin Interneurons and Hypoxia

PV-INs have unique energy requirements that make them especially susceptible to inflammation, as detailed in Chapter 2. Pro-inflammatory stimuli that are known to injure PV-INs include lipopolysaccharide, ketamine, and hypoxia [9, 24, 25]. Chapter 3 of this dissertation is describing work that explores the nature of PV-IN vulnerability in the context of exposure to chronic hypoxia or normoxia. These experiments utilized the PV^{cre}-tdTomato mouse line. The use of this mouse line, for the first time, allowed death of PV-INs to be distinguished from modulation of parvalbumin protein levels within PV-INs, as PV-INs can be identified in PV^{cre}-tdTomato mice independently of the presence of parvalbumin protein. We found that exposure to chronic hypoxia injured PV-INs but did not cause them to degenerate. Additionally, we found that calretinin interneurons, another class of inhibitory interneurons found in the brain, were not injured in response to chronic hypoxia. These experiments provide further evidence that, even when compared with another class of interneurons, PV-INs are uniquely vulnerable to inflammation.

1.5 Relationship Between Parvalbumin Interneurons and NMDA Receptors

Chapter 4 of this dissertation is a published article documenting our conversion of human neural progenitor cells to neurons that contain functional NMDA receptors. PV-INs depend on NMDA receptors to function properly. NMDA receptors in PV-INs regulate gamma oscillations and cognitive behaviors that include associative learning and working memory [26]. When the NMDA receptor 1 subunit was selectively ablated in PV-INs, phenotypes similar to those found in autism spectrum disorder and a change in gamma-band cross-frequency coupling were observed [27, 28]. A decrease in parvalbumin immunoreactivity

within PV-INs was observed when NMDA receptors were blocked [29]. Blocking NMDA receptors also reduces PV-IN excitation [30]. Decreased parvalbumin immunoreactivity within PV-INs and reduced PV-IN excitation are both markers of PV-IN injury. The relationship between PV-INs and NMDA receptors is discussed further in Chapter 2.

1.6 Importance of Using Human Neurons

It is noteworthy that the converted neurons were derived from human neural progenitor cells, as there are important differences between rodent and primate neurons. These differences are detailed in Chapter 4, but one key difference is that a short isoform of the NMDA receptor 2A subunit is found in primate but not rodent brain [31]. Since NMDA receptors that contain the NMDA receptor 2A subunit promote PV-IN maturation [32], it is possible that the presence of the short isoform of the NMDA receptor 2A subunit within PV-INs could change the results of an experiment. This is just one of many reasons why any results obtained from rodent experiments should be verified in a human-based model if possible.

1.7 Relationship Between NMDA and Inflammation

While NMDA receptor blockade is presented as pro-inflammatory in this dissertation, there are reports in the literature where blocking NMDA receptors attenuates inflammation and where NMDA itself is pro-inflammatory. The NMDA receptor antagonists ketamine and AP5 inhibited inflammation that was induced by lipopolysaccharide in a microglial cell line [33], and the NMDA receptor antagonist memantine attenuated inflammation in an atherosclerotic cell model [34]. Intraocular injections of NMDA in mice resulted in the

upregulation of pro-inflammatory cytokines [35]. It is well established that excitotoxicity can occur when NMDA receptor activation is prolonged, resulting in excessive calcium influx and an increase in pro-inflammatory cytokines [36, 37]. Whether NMDA receptor blockade is pro-inflammatory or anti-inflammatory is clearly dependent on the experimental model used and NMDA receptor antagonist dosage.

1.8 Concluding Thoughts

PV-INs are critical for proper brain function. PV-IN-related changes are found in so many diseases and disorders, including neurodegenerative and psychiatric diseases, and are linked to brain malfunction. As discussed in detail in Chapter 5, reduced parvalbumin protein expression can result in PV-IN injury, so parvalbumin is both a driver of and a marker of PV-IN health. Finding strategies to protect PV-INs and reduce their vulnerability should be of importance to anyone interested in lessening one small but clinically relevant aspect of any disease or disorder where PV-IN-related changes have been observed. It is my sincere hope that some of the knowledge gained from my dissertation experiments could one day play a small role in positively impacting treatment options for patients with diseases such as schizophrenia and Alzheimer's disease.

CHAPTER 2

This chapter is adapted from "Parvalbumin interneuron vulnerability and brain disorders", published in Neuropsychopharmacology in 2021, and has been reproduced with the permission of the publisher, Springer Nature, and my co-authors, Laura L. Dugan and Christine Konradi.

Parvalbumin Interneuron Vulnerability and Brain Disorders

2.1 Parvalbumin Interneurons Are Implicated in a Variety of Neuro-psychiatric Disease States

Injury to, or dysfunction of, parvalbumin inhibitory interneurons (PV-INs) has been proposed to contribute to the pathophysiology of several important neuro-psychiatric disorders, including schizophrenia, autism spectrum disorder (ASD), bipolar disorder (BPD), various neurodegenerative diseases, and even aging-related cognitive changes. In this review, we will briefly summarize the literature implicating PV-IN deficits in neuro-psychiatric conditions and discuss specific properties of these neurons that may make them selectively vulnerable to multiple stressors, including the complex developmental pathways required for normal development of PV-INs and circuits. Emerging literature suggests that approaches to preserve function of these unique inhibitory neurons have benefits for both acute and chronic brain disorders.

Extensive accounts in the literature point to PV-IN-related changes in individuals with schizophrenia [10-13], a finding that is supported by various animal models that recapitulate aspects of the disease [38-40], (Table 2.1). In schizophrenia, lower levels of PVALB mRNA, the gene coding for PV, were seen in the hippocampus and layer 4 of the dorsolateral prefrontal cortex, which might be partially explained by DNA

PV Alteration	Described in	References
Reduced number of PV-INs in medial prefrontal cortex	Animal models	[12, 14]
Reduced number of PV-INs in hippocampus	*) SZ; animal models	[10, 39-41]
Reduced number of PV-INs in caudal entorhinal cortex	SZ	[42]
Reduced number of PV-INs in parasubiculum	SZ	[42]
Reduced PV immunoreactivity in PV-INs in prefrontal cortex	Animal model	[9, 43]
Reduced PV immunoreactivity in anterior cingulate cortex	Animal model	[44]
Reduced PV mRNA expression in hippocampus	SZ	[10]

Reduced PV mRNA expression in prefrontal cortex	SZ	[45, 46]
Reduced excitatory synapse density on PV-INs	SZ	[47]
Decreased density of PV-INs expressing GluN2A mRNA in prefrontal cortex	SZ	[48]
Increased PV methylation in hippocampus	SZ	[19]
Increased gamma oscillatory activity during working memory	SZ	[49]
Gamma power deficit in medial prefrontal cortex	Animal model	[38]
Decreased perineuronal net labeling around PV-INs in dorsolateral prefrontal cortex	SZ	[43]

*) SZ = schizophrenia, human subject studies

Table 2.1. PV-IN alterations in schizophrenia and associated animal models

hypermethylation [10, 19]. Reductions in the number of PV-INs were reported in the hippocampus, entorhinal cortex, and subicular areas [10, 42, 45, 46]. Furthermore, individuals with schizophrenia have a lower density of excitatory synapses on PV-INs [47] and exhibit alterations in gamma oscillations during a working memory task [49]. Animal models that mimic schizophrenia replicate the loss of PV-INs in the hippocampus [39, 41, 50], and show a loss of PV fluorescence per cell in prelimbic regions [9]. Interestingly, early intervention during the prepubertal period might prevent loss of PV-INs, as shown in the methylazoxymethanol acetate (MAM) rat model of PV-IN loss in the ventral hippocampus [51]. While these findings point to a pathology in PV-INs, they cannot differentiate between loss of neurons or loss of PV expression. Some human and animal model data suggest that formerly PV-INs are still present but cease to express PV, though a definitive conclusion cannot be drawn at this point [14, 40, 43, 52].

Alzheimer's disease (AD) is also associated with changes in fast-spiking interneurons (Table 2.2). Transgenic mice with AD-like pathology were found to have reduced gamma power that, in one model, precedes cognitive impairment and amyloid plaque formation [53, 54]. Interestingly, amyloid plaques were reduced when hippocampal PV-INs artificially produced gamma oscillations in optogenetics paradigms [53]. Theta-gamma oscillation phase-amplitude cross-frequency coupling was impaired prior to neuronal loss or maximum tau pathology in a tau seeding model with AD-like pathology [55]. Evoked gamma oscillations to auditory stimuli were also disrupted in this model [55]. Separately, a voltage-gated sodium channel ($Na_v1.1$) that is largely found on axons of PV-INs was decreased in a mouse model with amyloid pathology, and in AD patients [56-58]. Restoration of the levels of this voltage-gated sodium channel increased gamma oscillations, while memory deficits and premature deaths decreased [58]. Furthermore,

PV Alteration	Described in	References
Reduced number of PV-INs in hippocampus	Animal model	[59]
Increased number of PV-INs in hippocampus	Animal model	[60]
Reduced number of PV-INs in parasubiculum	Animal model	[59]
Increased number of PV-INs in piriform cortex	*) AD	[16]
Reduced septohippocampal pathway synapse density on PV-INs	Animal model	[54]
PV-INs exhibit more depolarized resting membrane potentials and smaller action potential amplitudes	Animal model	[58]

Reduced hippocampal gamma power	Animal model	[53]
Reduced gamma activity	Animal model	[54, 58]
Impaired theta-gamma oscillation phase-amplitude cross-frequency coupling	Animal model	[55]
Disrupted evoked gamma oscillations to auditory stimuli	Animal model	[55]
Decreased number of neurons with intact perineuronal nets	AD	[15]

*) AD = Alzheimer's disease, human subject study

Table 2.2. PV-IN alterations in Alzheimer's disease and associated animal models

abnormalities in the default mode network, which is regulated in part by PV-INs [61], have been observed in AD patients [62-66].

Reports of changes of PV-INs in AD are not without controversy. For example, decreases in the number of PV-INs in the hippocampus were observed in two mouse models of AD [59, 67], while an increase in hippocampal PV immunoreactivity was observed in another [60], and no change in the number of hippocampal PV-positive interneurons was observed in yet another model [68]. These contradicting observations may be explained by the different mouse models used in each study. In AD patients, however, a decrease in PV-INs was reported in the dentate gyrus, and an increase in PV-INs was reported in the piriform cortex [15, 16, 67]. The different findings reported in each study could be due to the different brain regions examined. Indeed, it would be surprising to find that PV-IN densities in disease are uniform across every brain region given that fast-spiking interneurons have different functions in different brain areas.

ASD shares many overlaps with schizophrenia, not just on a clinical scale, but also with similar PV-IN abnormalities [69]. The Df(16)A+/− transgenic mouse and the LgDel(+/-) mouse, both of which model the 22q11.2 deletion in humans [38, 70-73], the contactin associated protein 2 (CNTNAP2) mouse [74-76], the neurexin transgene model [77], Shank models [14, 78-80], and platelet-derived growth factor receptor-beta (Pdgfrb) knockout mouse [81, 82] are examples of models for both ASD and schizophrenia, which have large effects on PV-IN function. In other mouse models of ASD, a reduction in PV-INs or a decrease in PV immunoreactivity has been reported [14]. Concurrently, PV knockout mice display behavioral phenotypes that resemble core behavioral phenotypes found in humans with ASD [83]. One of the best described ASD models, knock-out of the gene responsible for Rett syndrome, methyl CpG binding protein 2 (Mecp2), shows repetitive behaviors and

stereotypies even if the gene is selectively removed from INs only [84].

Schizophrenia also shares significant overlap with BPD [85, 86], including PV-IN pathology. Mouse models relevant for both disorders, including the disrupted in schizophrenia 1 gene (Disc1) [87-91], or brain derived neurotrophic factor (Bdnf) [92], show abnormal PV-IN function ranging from migration deficits to reduction in IN number.

But schizophrenia, AD, ASD, and BPD are not the only diseases for which PV-INs seem to play an important role. Epilepsy [93, 94] and prion disease [95] are among other disorders that are associated with alterations in PV-INs. There is therefore ample evidence that PV-INs are vital for brain function and intricately linked to brain malfunction.

2.2 Characteristics of PV-INs

Inhibitory GABAergic interneurons can be classified based on their co-expression of a variety of small proteins that principally function as neuromodulators or as calcium (Ca^{2+}) – binding proteins [5]. The Ca^{2+}-binding protein PV ("small albumin"), which is approximately 12kD in humans, defines one class of GABAergic interneurons. PV increases the rate of Ca^{2+} sequestration, reduces presynaptic Ca^{2+} levels, modulates short-term synaptic plasticity, and prevents cumulative facilitation (Figure 2.1), [96, 97]. Since PV rapidly sequesters Ca^{2+}, it strongly attenuates the Ca^{2+} -activated potassium conductance responsible for post-spike hyperpolarization, which explains in part why PV-INs repolarize faster and fire faster than other neurons. For this reason, the characteristic phenotype of PV-INs is fast-spiking action potentials at high energetic costs [5].

PV-INs in the cortex are highly interconnected via electrical and chemical synapses [98]. These networks are associated with plasticity from early life throughout

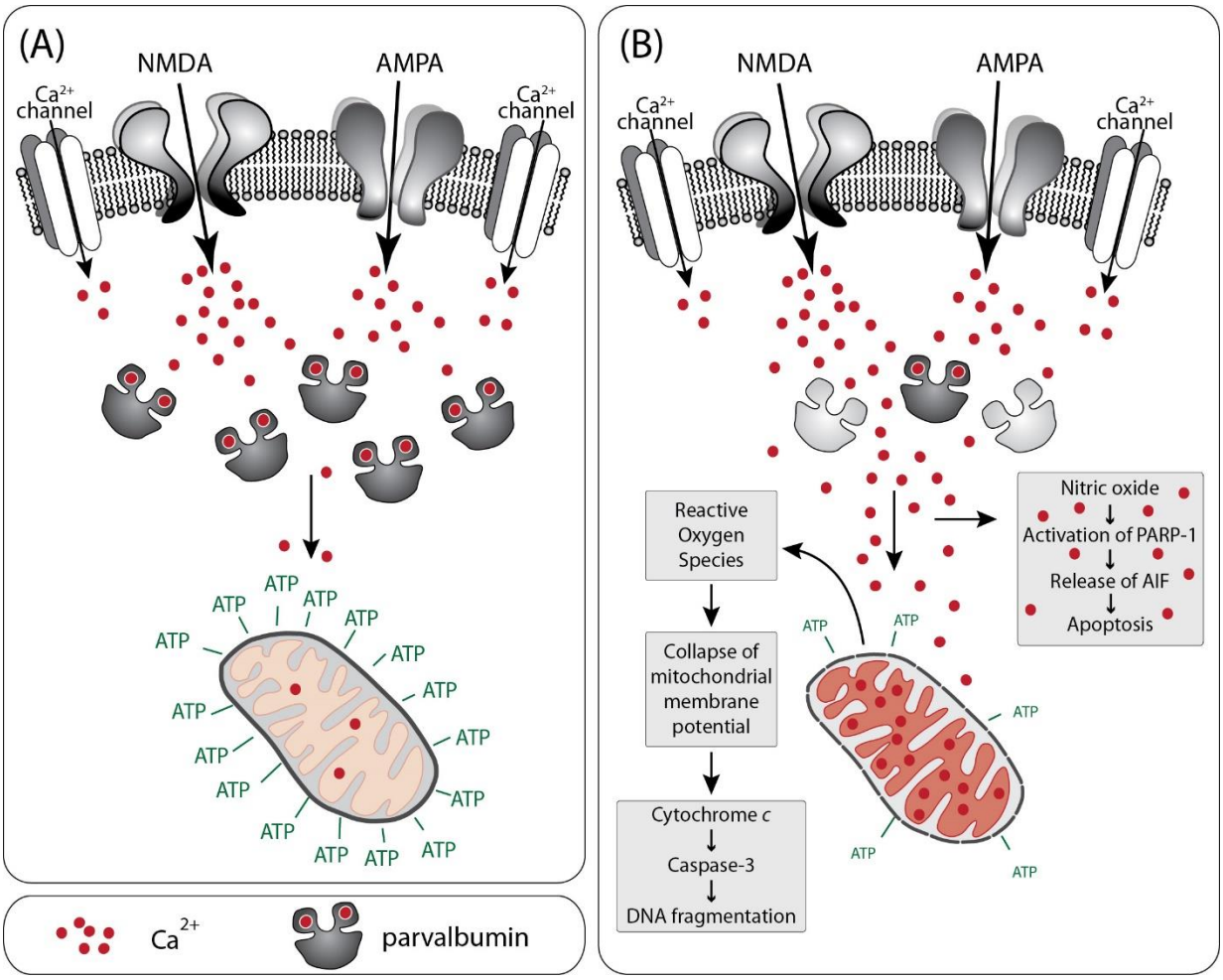

Figure 2.1. Parvalbumin protects mitochondria from Ca^{2+} overload. (A) Under physiological PV concentrations, Ca^{2+} entering through receptors and channels will be buffered by PV. Ca^{2+} in mitochondria remains at physiological levels, promoting ATP production. (B) Loss of PV leads to toxic accumulation of Ca^{2+} in mitochondria. High levels of Ca^{2+} disrupt the mitochondrial membrane potential and the electron transport chain. The resulting increase in reactive oxygen species causes the collapse of the mitochondrial membrane potential, release of cytochrome *c*, and activation of apoptotic pathways. Moreover, high cytosolic levels of Ca^{2+} activate neuronal nitric oxide synthase and increase nitric oxide levels. Nitric oxide can initiate another apoptotic pathway.

adulthood [99-102]. PV-INs have roles in both feedforward and feedback inhibition, regulation of sensory responses, and in learning and plasticity [5]. Individual PV-INs contact nearly every local pyramidal neuron which enables them to synchronize networks [103]. They help to create and maintain gamma oscillations, which are high-frequency waves between 20-100 Hz [5, 104]. Stimulation of PV-INs leads to an increase in gamma oscillation patterns, while inhibition of PV-INs or downregulation of PV at cortical synapses reduces gamma oscillations [105-107]. Gamma oscillations in humans are also associated with increased working memory load [108]. Animal studies suggest that a key mechanism of neural oscillations is through glutamatergic regulation. Indeed, PV-INs receive the greatest excitatory input of any population of inhibitory neurons in the cortex, which puts them under intense stress [9, 109].

2.3 PV-INs Have Unique Energy Requirements That Render Them Vulnerable to Many Stressors

PV-INs have extraordinary energy requirements to support a high metabolic activity and to protect against significant glutamatergic stress [9, 109, 110]. The large amounts of ATP needed to sustain gamma oscillations are supplied by a high density of mitochondria [110-112]. Studies have shown that the rate of oxygen consumption during hippocampal gamma oscillations can be equivalent to the rate of oxygen spent during a seizure [112, 113]. A substantial quantity of cytochrome *c* and cytochrome *c* oxidase supports the high bioenergetic needs of PV-INs [110, 114], but comes at a price as cytochrome *c* is also central to the induction of apoptosis [115].

The high metabolic activity of PV-INs is not only explained by their physiological characteristics, but by their structural characteristics as well. In CA1 of the rat

hippocampus, PV-INs have larger dendritic trees and thicker dendrites than calbindin- or calretinin-positive interneurons [109]. PV-INs have a higher density of inputs, more excitatory and inhibitory synapses, and a higher ratio of inhibitory to excitatory inputs than calbindin- and calretinin-positive interneurons [109]. Additionally, PV-INs connect to many principal neurons [103, 104, 116, 117]. They synchronize principal neuron activity [118] and they have a great impact on the energy-intensive processes of information selection and noise removal [5, 119]. In the MAM model of schizophrenia, reduced expression of PV-INs has been correlated with a reduction in coordinated neuronal activity during task performance in rats [39]. This observation provides a hypothesis about how loss of PV-INs might contribute to behavioral and clinical observations in neuro-psychiatric disorders.

The energy requirements of PV-INs make them highly susceptible to loss of mitochondrial membrane potential (a component of, and a proxy for, a decrease in mitochondrial function), and to metabolic and oxidative stress that accompanies disease states [110, 120]. In rodent models that recapitulate aspects of brain disorders, higher oxidative stress consistently correlates with decreased PV-positive cortical interneurons [44, 121]. In the hippocampus, oxidative stress was associated with a decrease in PV-INs as well as a reduction in gamma oscillations [122]. Conversely, in animal models where no change in oxidative stress was observed, PV-positive interneuron number was not changed [121].

The energy requirements of PV-INs also make them highly susceptible to inflammation. For example, the NMDA receptor antagonist ketamine, a pro-inflammatory stimulus, injures PV-INs *in vitro* and *in vivo* [9, 123]. This injury is connected to IL-6-mediated Nox2-dependent NADPH oxidase activation and production of superoxide [9, 123]. IL-6 is likely signaling through STAT3 [124]. STAT3 can directly regulate mitochondrial

function [125, 126], and Nox2 can modulate mitochondrial activity [127-129]. Since PV-INs have many mitochondria, inflammatory stimuli that negatively affect mitochondrial activity and function would negatively affect PV-IN health.

2.4 Excitatory Drive onto Parvalbumin Interneurons Contributes to Their Vulnerability

The strong excitatory drive of PV-INs is mediated by Ca^{2+}-permeable AMPA receptors as well as NMDA receptors [130-132]. While NMDA receptors are the primary source of dendritic Ca^{2+} in many cell types, in PV-INs dendritic Ca^{2+} enters through both NMDA receptors and Ca^{2+}-permeable AMPA receptors (Figure 2.1), [133]. PV-INs have faster Ca^{2+} influx kinetics than other cell types in part because of Ca^{2+}-permeable AMPA receptors [133]. Ca^{2+}-permeable AMPA receptors are required for long-term potentiation in PV-INs, as excitatory post-synaptic currents are reduced when Ca^{2+}-permeable AMPA receptors are blocked [134, 135].

While Ca^{2+} homeostasis is an important factor in regulating mitochondrial activity and function, Ca^{2+} -permeable AMPA receptors in PV-INs also lead to vulnerability [136]. Rapid Ca^{2+} influx through AMPA receptors can lead to a pathological accumulation in the mitochondrial matrix, particularly if PV levels are reduced (Figure 2.1B), [137]. If the pathological threshold is crossed, the electron transfer chain is disrupted, reactive oxygen species accumulate, the permeability transition pore opens, the outer mitochondrial membrane ruptures, cytochrome *c* is released, and an apoptotic cell death program is activated [115, 137]. The combination of large Ca^{2+} waves, high mitochondrial density, and dependence on uninterrupted ATP supply creates a delicate balance in PV-INs that can rapidly turn into pathology. Even slower, consistent Ca^{2+} influx through Ca^{2+}-permeable

AMPA receptors can be damaging via activation of neuronal nitric oxide synthase and generation of nitric oxide and resultant activation of Poly(ADP-ribose) polymerase 1 (PARP-1), (Figure 2.1B), [137, 138]. PARP-1 leads to the release of apoptosis-inducing factor (AIF) via a nuclear signal that proliferates to mitochondria [138].

Ca^{2+}-permeable AMPA receptors are a major entry point of zinc [139-141]. Like Ca^{2+} influx, zinc influx into neurons leads to the generation of nitric oxide and subsequent activation of PARP-1 and cell death [142]. Zinc is more potent than Ca^{2+} in its ability to disrupt mitochondrial function [137]. Unlike Ca^{2+}, the influx of zinc through Ca^{2+}-permeable AMPA receptors can lead to a *long-lasting* production of superoxide in mitochondria [140]. At equivalent concentrations, zinc induces a larger increase in cytochrome *c* and AIF than Ca^{2+} [143]. Consistent with the notion that the presence of Ca^{2+}-permeable AMPA receptors contributes to the vulnerability of PV-INs, blocking of these receptors attenuates cortical neuron death in an *in vitro* model of traumatic brain injury; attenuates hippocampal pyramidal neuron loss in a mouse hippocampal slice model of oxygen-glucose deprivation; and attenuates retinal ganglion cells loss in a rat model of glaucoma [139, 144, 145].

The majority of PV-INs in humans and monkeys express NMDA receptors [146, 147]. The ratio of GluN2A-containing NMDA receptors to GluN2B-containing NMDA receptors is five times higher in cultured PV-INs than in pyramidal neurons, and GluN2A-containing NMDA receptor activity is critical for the preservation of PV immunoreactivity in cultured PV-INs [29]. Importantly, NMDA receptors in PV-INs are regulating gamma rhythms and cognitive behaviors [26].

The dependence of most PV-INs on NMDA receptor function presents another

vulnerability. In schizophrenia, NMDA receptors are believed to be hypo-functioning, and the inhibition of NMDA receptors recapitulates many of the symptoms of schizophrenia [30, 132, 148]. NMDA receptor antagonists, such as ketamine and phencyclidine, can transiently reproduce key clinical features of schizophrenia, and are believed to reduce PV-IN excitation [30]. Working memory is notably impaired in schizophrenia and in other neuro-psychiatric diseases likely due to the expected change in gamma oscillation power resulting from disinhibition [30], in line with transgenic mouse studies in which NMDA receptors are genetically removed in PV-INs [26]. Recent evidence in rats suggests that working memory is dependent on GluN2A-containing NMDA receptors in the prefrontal cortex [149]. Administration of a GluN2A-selective NMDA receptor antagonist caused an abnormal increase in gamma power, while administration of NMDA receptor antagonists that are selective for other subunits resulted in little-to-no change [150]. Human brains from individuals with schizophrenia have a lower density of GluN2A-expressing PV-INs in layers 3 and 4 of prefrontal cortex compared to the brains from a control group [48]. When this evidence is combined with the finding that gamma oscillations correlate with working memory load in humans, it is likely that the decreases in working memory that are observed in diseases such as schizophrenia are in part mediated by the decrease in glutamatergic inputs through GluN2A-containing NMDA receptors onto PV-INs.

2.5 The Developmental Trajectory of Interneurons Introduces Unique Vulnerabilities

Like other interneurons, PV-INs are derived from progenitor cells in the embryonic ganglionic eminences of the ventral telencephalon of the developing brain (Figure 2.2). Their ‘parvalbumin’ fate seems to be established at their origin, as the progenitors leave the cell cycle [151, 152]. Once postmitotic, cells migrate tangentially toward cortical areas

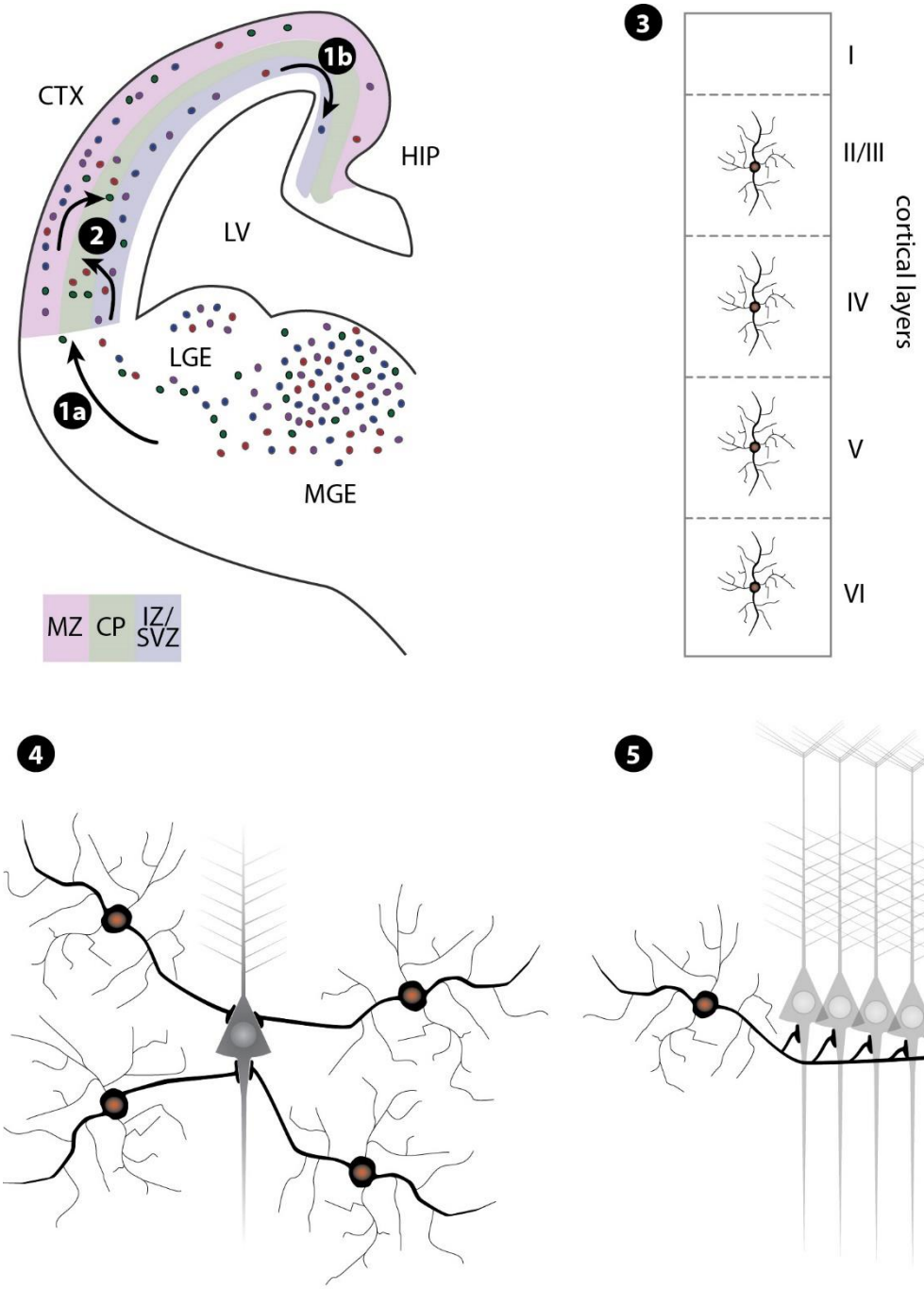
CTX
1b
HIP
LV
2
LGE
1a
MGE
MZ
CP
IZ/
SVZ
3
I
II/III
IV
V
VI
cortical layers
4
5

Figure 2.2. Development of cortical interneurons. The majority of interneurons are derived in the medial and lateral ganglionic eminence (MGE; LGE) from where they migrate tangentially along the marginal zone (MZ) and intermediate zone (IZ)/subventricular zone (SVZ) of the developing cortex, (1a). Most PV-INs are derived from the ventral MGE, and their 'parvalbumin' fate seems to be established at their origin, as the progenitors leave the cell cycle. Interneurons migrate through the cortex in a lateral-to-medial tangent, with the hippocampus among the last areas to be settled (1b). To enter the developing cortical plate (CP), interneurons have to switch their mode of migration from tangential to radial (2). PV-INs colonize the cortex in an inside-out fashion, by which layers VI/V are colonized first, followed by layers IV, III and II. In the adult brain, parvalbumin interneurons are found in all cortical layers except layer I (3), and in the hippocampal pyramidal layer. As the final step, interneurons have to build synaptic networks with pyramidal neurons and other interneurons (4). Parvalbumin neurons synapse onto pyramidal neurons at the cell body and the axon hillock, and thus exert control over information outflow. Network activity is synchronized by individual interneurons contacting nearly every local pyramidal neuron (5). LV – lateral ventricle; CTX – cortex; HIP – hippocampus

and then radially into pre-determined cortical layers (Figure 2.2, steps 1a, 1b, and 2), [153, 154]. During migration, cell-intrinsic programs and external cues must be coordinated in a time- and location-sensitive manner [155]. Externally, an exquisite coordination of attractant and repellant guidance factors transmitted from various brain regions guide migrating neurons to their ultimate destination [156]. Intracellularly, an expression of responsive receptors on the neurons must be timed with the transmission of guidance factors from remote brain tissues. These receptors activate intraneuronal signaling cascades that dynamically remodel microtubule and actin cytoskeletal components to extend and retract processes that move the cells toward their destination [157]. As interneurons assume their final position within a specific region and layer of the cortex and hippocampus, they have to switch to a molecular program designed to establish axon pathfinding and synaptic connections with local excitatory neurons born in the subventricular zone, and with other interneurons that had migrated from areas deep inside the developing brain (Figure 2.2, steps 3 and 4), [153, 154]. PV-INs colonize the cortex in an inside-out fashion, by which layers VI/V are colonized first, followed by layers IV, III and II [158].

Migration of interneurons and incorporation into the local environment constitute times of high vulnerability. During mouse brain development, the fraction of GABAergic interneurons to glutamatergic neurons is constant from early corticogenesis throughout brain development and into the adult brain [159]. Any disruption during migration can not only leave interneurons in the wrong location, as has been shown in schizophrenia [160-162], but also have permanent consequences on the ratio of specific neuron types. The characteristics of the large number of interneuron types with diverse transcriptional signatures are not random but rather predetermined at the earliest developmental stages [151, 152, 154]. Such an early determination of fate would limit their ability for self-

renewal or de-differentiation if damaged during migration. The hippocampus is the farthest brain area reached by interneurons, and as such has the longest developmentally open window, with the highest likelihood to be affected by deleterious impacts on migration [163]. The preponderance of interneuron pathologies in the hippocampus and adjacent cortical areas, such as the interneuron pathologies observed in schizophrenia and BPD, might be, at least in part, a reflection of this extended developmental vulnerability [10, 42, 148, 164-166].

Taken together, for cells to find their proper location and integrate into the local neuronal network, intrinsic programs that determine interneuron cell-type, timing and response to guidance factors, cytoskeletal reorganization, migration, and connection to synaptic partners, have to be coordinated with external cues, which themselves are subject to intrinsic programs in distant cell types. It seems almost beyond a miracle of nature for this process to work correctly, and yet in most cases it succeeds. While there likely is some space to correct for minor variabilities, it seems reasonable to assume that the process also has some vulnerabilities.

2.6 Conclusion and Future Directions

PV-INs are important for proper brain function. Their ontogeny and physiological properties render them uniquely susceptible to environmental disturbances. This vulnerability contributes to their role in numerous brain disorders. PV-INs are implicated in neurodevelopmental diseases such as early-onset psychiatric disorders and in neurodegenerative diseases such as Alzheimer's disease, demonstrating the vulnerability of this interneuron subset throughout life. Therapeutic strategies to protect PV-INs from injury should be explored to prevent and/or lessen their role in the various brain disorders

in which dysfunctional PV-INs are implicated. For example, recently discovered GluN2A-selective NMDA receptor positive allosteric modulators could help to restore normal gamma oscillations and improve working memory in patients with schizophrenia, as these compounds should selectively target PV-INs [167, 168].

New approaches should also be explored to better understand PV-IN vulnerability. Human PV-INs can be derived from induced pluripotent stem cells to examine metabolism, genetics, physiology, and responses to stress. Novel mouse models, including models that label PV-INs with tdTomato such as [169], can be exposed to various conditions to differentiate between loss of neurons and loss of PV expression. Imaging modalities, including functional magnetic resonance imaging, can be used to observe the integrity of PV-IN-containing circuits in forebrain and hippocampus in humans with disease compared to healthy controls. We will soon have a greater understanding of PV-IN vulnerability because of the novel tools at our disposal.

CHAPTER 3

Selective Vulnerability of Hippocampal Parvalbumin Interneurons in a Sustained Hypoxia Mouse Model Reflects Injury but Not Overt Neurodegeneration

3.1 Introduction

Hypoxia is a common condition which occurs in many disease states, including chronic obstructive pulmonary disease (COPD), pneumonia, and exposure to high altitude [170]. Individuals with prolonged hypoxia often exhibit progressive organ dysfunction [170], but among the most devastating consequences of sustained hypoxia are changes in central nervous system (CNS) function that can include impaired cognition, hallucinations, seizures, and even coma. Many of these CNS deficits persist after normalization of oxygen levels, but the processes which lead to sustained CNS effects of hypoxia remain incompletely understood.

Hypoxia is defined generally as a state of low oxygen [171-173] that is known to induce inflammation [174]. Hypoxia has many effects within the brain, including on astrocytes, microglia, and neurons. Astrocytes specifically may function as “hypoxia sensors,” sensing decreased oxygen and increased carbon dioxide (hypercarbia, which frequently accompanies hypoxia), and these events in turn trigger increased intracellular calcium in astrocytes [175]. Microglia are activated in response to hypoxia as well, resulting in the release of factors such as glutamate, inflammatory cytokines, nitric oxide, and reactive oxygen species [176-178].

Hypoxia therefore engages both metabolic and inflammatory stressors. Among the neuronal populations which are known to have susceptibility to such stress are the parvalbumin inhibitory interneurons (PV-INs). PV-INs have many critical functions, including the

generation and maintenance of gamma oscillations that are important for working memory [5, 104, 108]. The loss of PV-INs in the prefrontal cortex in response to hypoxia has been reported [24, 179-183]. Treatment with apocynin, a NADPH oxidase (NOX) inhibitor, or being raised in an enriched environment, can prevent this PV-IN loss [24, 181-183]. However, it is not yet known whether PV-INs are dying, or whether the interneurons are losing their namesake protein yet remaining alive, as PV-IN loss has traditionally been determined via immunohistochemistry.

In this study, we used chronic exposure to a hypoxic environment [184-188] to determine whether vulnerability of PV-INs reflected loss of the phenotypic protein marker alone, or frank degeneration of these neurons. To this aim, we exposed PV^{cre}-tdTomato mice to chronic hypoxia or normoxia for 24-26 days and found that exposure to chronic hypoxia injures hippocampal PV-INs but does not cause significant loss of these neurons.

3.2 Methods

3.2.1 Ethical Approval

All animal studies were approved by the Animal Care Program and IACUC at Vanderbilt University Medical Center and were in accordance with the PHS Guide for the Care and Use of Laboratory Animals, USDA regulations, and the AVMA Panel on Euthanasia.

3.2.2 Animals

Breeding pairs of the B6 PV^{cre} (strain # 017320) and Ai9 (strain # 007909) mouse lines were purchased from The Jackson Laboratory. Female B6 PV^{cre} mice were crossed with male Ai9 mice to generate mice that are heterozygous for the PV^{cre} knock-in allele and

heterozygous for the Rosa-CAG-LSL-tdTomato-WPRE conditional allele. These mice will be referred to as PV^{cre}-tdTomato mice. These mice exhibit tdTomato expression in PV-INs that is no longer regulated by the *Pvalb* promoter. tdTomato expression is driven by the Rosa26 promoter, which allows PV-INs to be identified even if *Pvalb* gene expression is modified by exposure to hypoxia. Experiments were performed on two independent cohorts of male and female PV^{cre}-tdTomato mice that were 14-17 months old at the time of blood collection and cardiac perfusion. Mice were randomized into normoxia and hypoxia groups.

3.2.3 Exposure to Normoxia and Hypoxia

Mice randomized to the hypoxia group were kept in a normobaric hypoxia (8% O_2) chamber (BioSpherix) for 24-26 days. Mice randomized to the normoxia group were transferred to the same housing facility as the mice in the hypoxia group and were maintained under normal animal housing conditions for 24-26 days.

3.2.4 Blood Collection and Processing

At the end of the hypoxic or normoxic exposure, mice were anesthetized with isoflurane. Blood was collected via the facial vein. Blood was incubated on ice for approximately 2 hours and centrifuged at 3,000 RPM for 30 minutes at 4°C. Serum was separated and stored at -80°C.

3.2.5 Cardiac Perfusion and Collection of Brain

At the end of the hypoxic or normoxic exposure (if blood was not collected) or after blood collection, mice were deeply anesthetized with isoflurane and then perfused transcardially with PBS followed by PBS containing 4% paraformaldehyde. Whole brains were removed and post-fixed in PBS containing 4% paraformaldehyde at 4°C overnight and then stored at 4°C in PBS containing 0.02% sodium azide. Brains were sliced on a Leica VT1000 S vibrating blade microtome into 50 µm sections. Sections were stored at -20°C in PBS containing 30% ethylene glycol, 30% glycerol, 20 mM potassium fluoride, 1 mM tetrasodium phosphate, and 1 mM sodium orthovanadate until being processed for immunostaining.

3.2.6 Immunostaining

Three hippocampal sections per mouse were chosen for parvalbumin immunostaining, one section corresponding to bregma ~-1.46 mm to ~-1.94 mm, one section corresponding to bregma ~-2.46 mm to ~-2.70 mm, and one section corresponding to bregma ~-2.92 mm to ~-3.16 mm. Two hippocampal sections per mouse were chosen for calretinin immunostaining, one section corresponding to bregma ~-1.46 mm to ~-1.94 mm and one section corresponding to bregma ~-2.46 mm to ~-2.70 mm. Sections were washed 3 times (5 minutes per wash) in PBS containing 0.1% Triton X-100 at room temperature on a rotator and then incubated in PBS containing 0.1% Triton X-100 and 10% normal goat serum for 1 hour at room temperature on a rotator. Sections were incubated in rabbit anti-parvalbumin (Swant, PV 27, 1:1,000 dilution) or rabbit anti-calretinin (Swant, CR 7697, 1:500 dilution) primary antibody made in PBS containing 0.1% Triton X-100 and 10% normal goat serum

at 4°C overnight on a rotator. Sections were washed 3 times (5 minutes per wash) in PBS containing 0.1% Triton X-100 at room temperature on a rotator and then incubated in goat anti-rabbit Alexa Fluor 488 secondary antibody (Invitrogen, A-11008, 1:1,000 dilution) made in PBS containing 0.1% Triton X-100 for 3 hours at room temperature. Sections were washed 3 times (5 minutes per wash) in PBS containing 0.1% Triton X-100 at room temperature on a rotator and then mounted using VECTASHIELD® HardSet™ Antifade Mounting Medium with DAPI (Vector Laboratories, H-1500-10).

3.2.7 Confocal Imaging

Z-stack tile scan images were acquired with an LSM 880/Axio Observer.Z1 confocal microscope (Zeiss) using the 40X water immersion objective. Confocal microscopy settings were kept constant for each series of immunostaining experiments. Experimenters were blinded during imaging.

3.2.8 Image Processing and Analysis

Interneurons were traced and measured using MetaMorph (Molecular Devices). Concordance between MetaMorph tracers was established. For slices immunostained with parvalbumin, with only the tdTomato channel turned on, tdTomato-positive objects (presumed PV-INs) in CA1 and CA3 of hippocampus were traced, and the average intensity and intensity signal: noise of the parvalbumin immunostaining channel of each tdTomato-positive object was logged. For slices immunostained with calretinin, calretinin interneurons in CA1 and CA3 of hippocampus were traced, and the average intensity of each calretinin

interneuron was logged. Concordance between the number of parvalbumin-containing presumed PV-INs and the number of presumed PV-INs was determined by dividing the number of tdTomato-positive objects with parvalbumin immunostaining channel signal: noise ≥1 by the total number of tdTomato-positive objects. Experimenters were blinded during image processing and analysis. The experimental code was only broken at the completion of all analysis to allow statistics to be performed.

3.2.9 Quantification of Blood IL-6 Levels

An IL-6 Mouse ProQuantum Immunoassay Kit (A43656, Invitrogen) was used to quantify mouse IL-6 protein in the collected serum according to the provided Product Information Sheet. Of note, 5 µL sample volumes were used, and the assay plate was incubated overnight.

3.2.10 Statistical Analysis

SigmaPlot 14.5 (Inpixon) was used to create all graphs and to perform all statistics. Mann-Whitney rank sum tests were performed for all Figures. Significant differences were noted if $P < 0.05$.

3.3 Results

3.3.1 Exposure to Chronic Hypoxia Increases Serum IL-6 Levels

PV^{cre}-tdTomato mice were exposed to chronic hypoxia or normoxia for 24-26 days. Using

a ProQuantum Immunoassay, we found that mice exposed to chronic hypoxia had elevated serum levels of the pro-inflammatory cytokine IL-6 (Figure 3.1). Increased levels of IL-6 suggested that chronic hypoxia did in fact induce inflammation in the mice.

3.3.2 Exposure to Chronic Hypoxia Results in PV-IN Injury but Not Degeneration

PV-INs are found in the hippocampus, a brain structure that is important for learning and memory, including working memory [5, 189]. PV-INs are thought to be important for encoding and retrieval of hippocampal-dependent memory, and selective vulnerability of PV-INs is thought to contribute to age-associated cognitive deficits [5, 6, 104]. We have previously demonstrated that IL-6 mediates age-related loss of hippocampal PV-INs [124]. To determine whether ongoing inflammation from chronic hypoxia may produce a similar injury, we analyzed parvalbumin protein expression in the CA1 and CA3 hippocampal regions of mice subjected to chronic hypoxia. We found that PV^{cre}-tdTomato mice exposed to chronic hypoxia had lower intensity of parvalbumin immunostaining within each presumed PV-IN in CA1 and CA3 of hippocampus (Figures 3.2A and 3.3A). A reduction in immunostaining intensity suggests that exposure to chronic hypoxia resulted in injury to hippocampal PV-INs. This analysis concurs with earlier unpublished data showing that C57BL/6 mice exposed to chronic hypoxia exhibited significant loss of parvalbumin immunoreactivity in CA1 and CA3 of hippocampus.

Additionally, PV^{cre}-tdTomato mice exposed to chronic hypoxia had lower concordance between the number of parvalbumin-containing presumed PV-INs and the number of presumed PV-INs in CA1 of hippocampus (Figures 3.2B and 3.3B). A decrease in concordance between PV-INs that contain parvalbumin and the total number of PV-INs

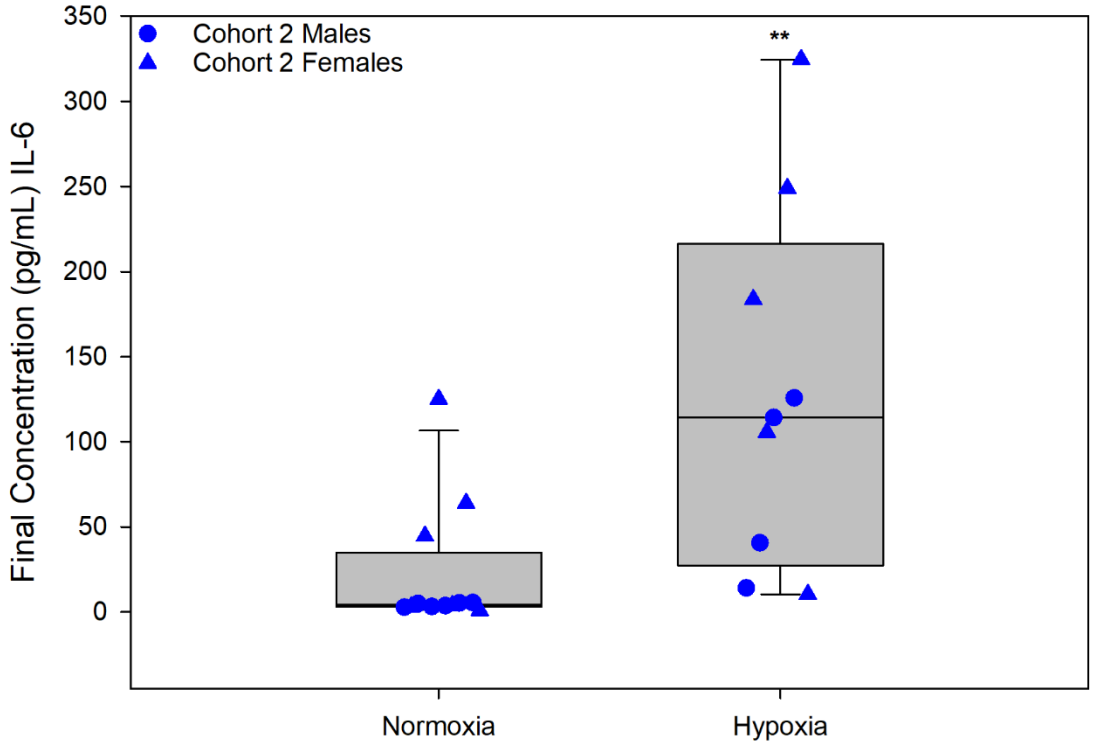

Figure 3.1. Prolonged hypoxia increases the pro-inflammatory cytokine IL-6. The serum concentration of IL-6 from PV^{cre}-tdTomato mice exposed to normoxia or hypoxia was graphed. The individual data points are spread slightly along the X-axis to allow each point to be better visualized. $^{**}P < 0.01$.

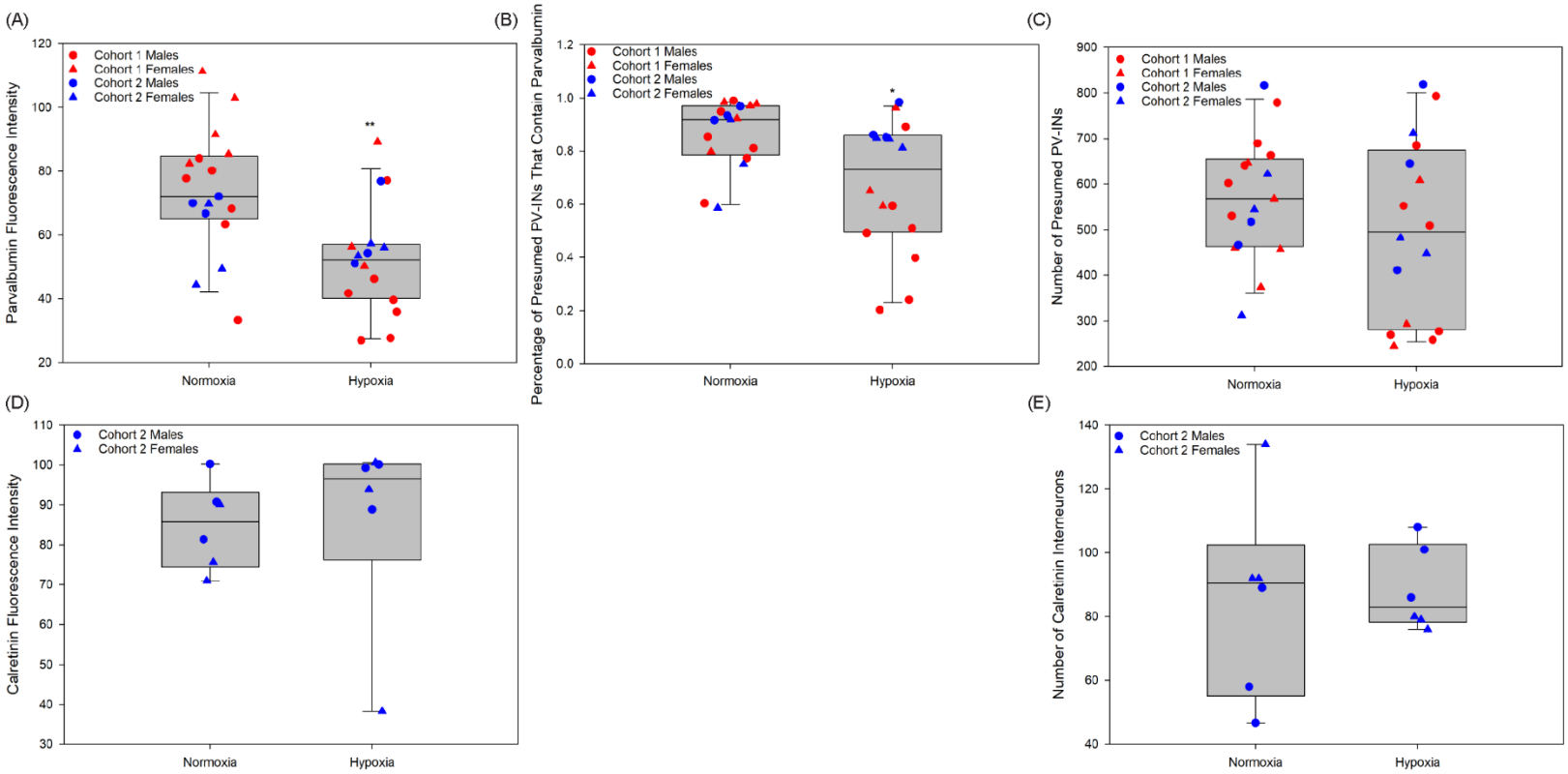

Figure 3.2. Effects of prolonged hypoxia on PV-INs and calretinin interneurons in CA1 of hippocampus. The intensity of parvalbumin immunostaining within each presumed PV-IN (A), percentage of presumed PV-INs that contain parvalbumin (B), number of presumed PV-INs (C), intensity of calretinin immunostaining within each calretinin interneuron (D), and number of calretinin interneurons (E) in CA1 hippocampal slices from PV^{cre}-tdTomato mice exposed to normoxia or hypoxia were graphed. The individual data points are spread slightly along the X-axis to allow each point to be better visualized. $^{**}P < 0.01$; $^{*}P < 0.05$.

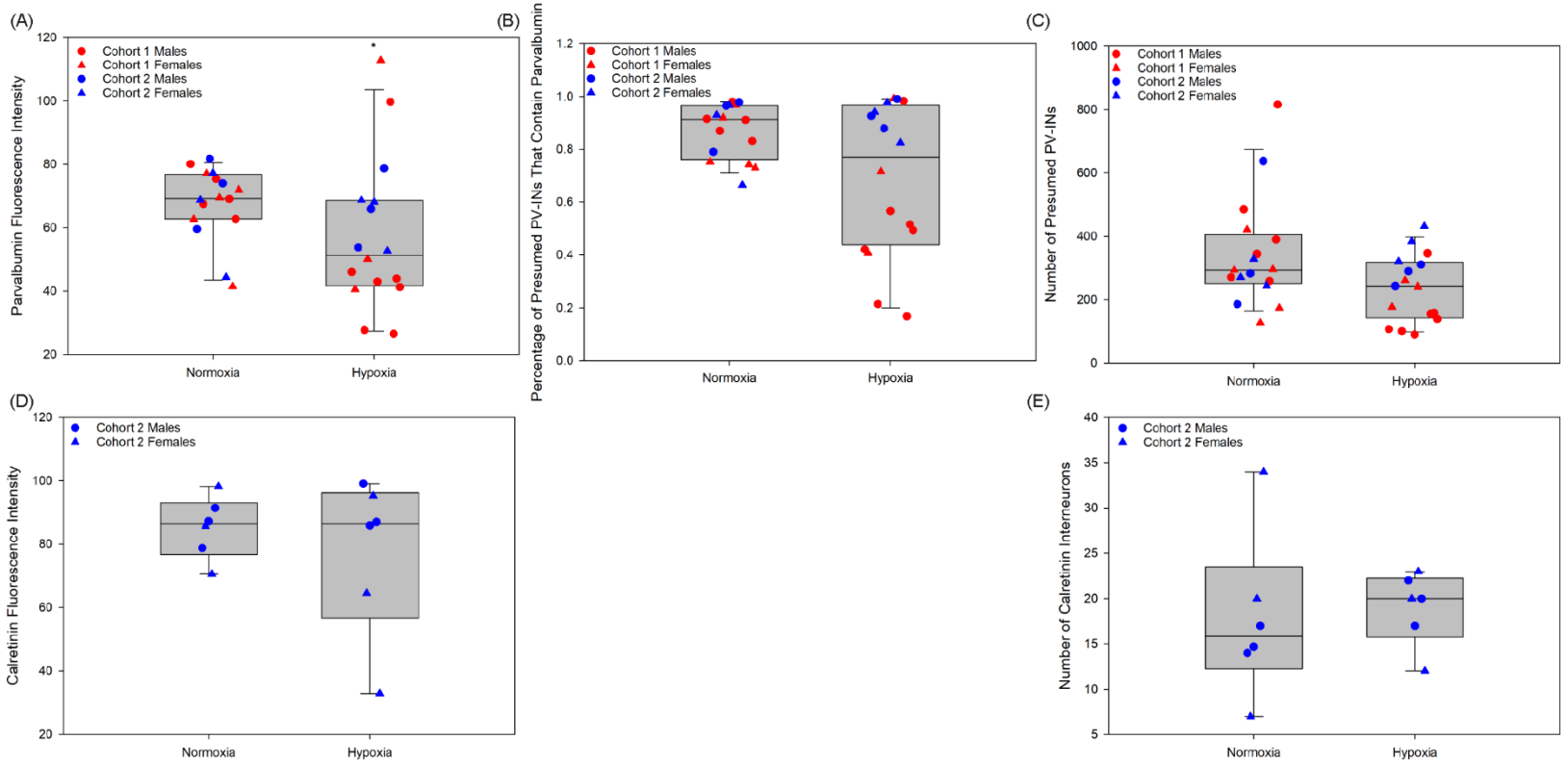

Figure 3.3. Effects of prolonged hypoxia on PV-INs and calretinin interneurons in CA3 of hippocampus. The intensity of parvalbumin immunostaining within each presumed PV-IN (A), percentage of presumed PV-INs that contain parvalbumin (B), number of presumed PV-INs (C), intensity of calretinin immunostaining within each calretinin interneuron (D), and number of calretinin interneurons (E) in CA3 hippocampal slices from PV^{cre}-tdTomato mice exposed to normoxia or hypoxia were graphed. The individual data points are spread slightly along the X-axis to allow each point to be better visualized. *$P < 0.05$.

provides further evidence to suggest that exposure to chronic hypoxia led to PV-IN injury.

However, mice exposed to chronic hypoxia had no difference in the number of presumed PV-INs in CA1 or CA3 of hippocampus (Figures 3.2C and 3.3C). A change in the number of PV-INs would be indicative of PV-IN degeneration, so this data suggests that PV-INs are not degenerating in response to chronic hypoxia. Taken together, this data indicates that chronic hypoxia leads to hippocampal PV-IN injury but not degeneration.

3.3.3 Exposure to Chronic Hypoxia Does Not Result in Calretinin Neuron Injury or Degeneration

To determine whether another class of interneurons was also vulnerable to the same hypoxic insult, we measured calretinin fluorescence intensity and the number of calretinin interneurons in the CA1 and CA3 hippocampal regions of mice subjected to chronic hypoxia. Mice exposed to chronic hypoxia had no difference in intensity of calretinin immunostaining in CA1 or CA3 of hippocampus (Figures 3.2D and 3.3D). This data suggests that hippocampal calretinin interneurons were not injured in response to chronic hypoxia. Mice exposed to chronic hypoxia also had no difference in the number of calretinin interneurons in CA1 or CA3 of hippocampus (Figures 3.2E and 3.3E), indicating that hippocampal calretinin interneurons did not degenerate in response to chronic hypoxia. In contrast to PV-INs, this data suggests that calretinin interneurons are not vulnerable to chronic hypoxia.

3.4 Discussion

Our group and others have reported on the selective vulnerability of subsets of inhibitory interneurons to both inflammatory and metabolic stress, with the PV-IN population being distinctly sensitive to these stressors. PV-INs are vulnerable to many stressors likely due to multiple unique properties of PV-INs, including their tonic firing activity, their strong excitatory drive, their unique energy requirements, extensive arborization, and neurotransmitter configuration, as well as their complex developmental trajectory [6]. Here, in contrast to prior work that could not determine whether injured PV-INs had degenerated, we have distinguished between PV-IN injury and degeneration by using PV^{cre}-tdTomato mice. Our data have revealed that sustained hypoxia, which we confirmed was pro-inflammatory, leads to PV-IN injury but not degeneration. We also show that another subset of interneurons, calretinin interneurons, are not injured in response to chronic hypoxia.

There are many interesting questions that these experiments have not answered. What would happen to PV-INs if the mice returned to normal housing for a given period of time after the chronic hypoxic exposure, prior to blood collection and perfusion? Depending on how long the mice were in normal housing after hypoxia, would the PV-INs remain injured? The Dugan Laboratory previously published on a different PV-IN injury model, where mice were injected with ketamine on two consecutive days and then perfused [9]. A decrease in parvalbumin fluorescence was observed in slices from the ketamine-injected mice [9]. They found that the loss of parvalbumin fluorescence in their model was reversible, as the difference in parvalbumin fluorescence between groups gradually lessened if the mice were perfused after 3 or 10 days after the injections [123]. It remains to be seen whether injured PV-INs would recover in our chronic hypoxia model if the mice spent time in normal housing after the pro-inflammatory insult. What if the mice were exposed to hypoxia for

longer than they were in these experiments, or if the hypoxic exposure was more severe than the 8% O_2 used for these experiments? Would a subset of hippocampal PV-INs degenerate? To my knowledge, since prior publications could not distinguish between PV-IN injury and degeneration, there is no prior data that could be used to form a hypothesis for what would happen to PV-INs in this scenario.

What is happening to PV-INs outside of the hippocampus? Entire mouse brains were sliced, and all sections were stored at -20°C in the ethylene glycol and glycerol-based solution described in Methods, so PV-INs from other brain structures from the same 2 cohorts of PV^{cre}-tdTomato mice exposed to chronic hypoxia or normoxia could be analyzed in future studies. Hippocampal PV-INs are fast-spiking, so it is possible that all fast-spiking PV-INs, regardless of what brain structure they are found in, could be injured but not degenerated in response to hypoxia. PV-INs in the prefrontal cortex are fast-spiking, and prior literature describes a loss of PV-INs in the prefrontal cortex [24, 179, 183]. As with other prior literature, however, loss of PV-INs is solely determined by loss of parvalbumin immunostaining in these studies, so it would be interesting to see whether PV-INs in the prefrontal cortex are injured but not degenerating in response to chronic hypoxia in PV^{cre}-tdTomato mice. Hippocampal PV-IN injury likely leads to impaired encoding and retrieval of hippocampal-dependent memory [5, 6, 104]. Injury to PV-INs in the prefrontal cortex may result in impaired working and spatial memory [183].

What is happening to PV-INs that are not fast-spiking, such as the multipolar bursting neurons that are parvalbumin-positive but not fast-spiking [190, 191]? The fast-spiking nature of the hippocampal PV-INs is likely to be responsible in part for why these neurons are vulnerable [6], so non-fast-spiking PV-INs may not be as injured in response to chronic hypoxia. However, if the presence of the parvalbumin protein itself is responsible in part for

PV-IN vulnerability, even in non-fast-spiking PV-INs, then non-fast-spiking PV-INs may indeed be injured in response to chronic hypoxia. Injury to the multipolar bursting neurons that are parvalbumin-positive but not fast-spiking may lead to impaired theta frequency oscillations [190].

What is happening to PV-INs that are excitatory, such as PV-INs in the ventral pallidum that project to glutamatergic neurons in the lateral habenula or that project to dopaminergic neurons in the ventral tegmental area [192, 193]? These excitatory PV-INs could feasibly have different properties than the canonical inhibitory PV-INs, which might render them less or more vulnerable to stressors such as chronic hypoxia. Injury to PV-INs in the ventral pallidum that project to glutamatergic neurons in the lateral habenula may result in a behavioral despair phenotype, while injury to PV-INs in the ventral pallidum that project to dopaminergic neurons in the ventral tegmental area may result in a social avoidance phenotype [193].

The question of what events are being triggered by sustained hypoxia, and whether treatments might be developed to prevent or reverse these changes, has taken center stage in the last two years due to the SARS-CoV-2 pandemic. There is clear evidence that a subset of those infected with COVID-19 present with hypoxia and associated cytokine release [194, 195]. There is a high likelihood that the injury process we observed after sustained hypoxia in PV-INs, a critical population of neurons, is occurring in COVID-19 patients. If this is occurring, appropriate anti-inflammatory strategies might be beneficial for COVID-19 patients who present with hypoxia, as these strategies could rescue their dysfunctional PV-INs. Whether in the context of COVID-19 or any other condition associated with hypoxia, the experiments described here highlight the importance of researching strategies to rescue injured PV-INs.

CHAPTER 4

This chapter is adapted from "Robust Expression of Functional NMDA Receptors in Human Induced Pluripotent Stem Cell-Derived Neuronal Cultures Using an Accelerated Protocol", published in Frontiers in Molecular Neuroscience in 2021, and has been reproduced with the permission of the publisher, Frontiers Media, and my co-authors, Mrinalini Dixit, José C. Zepeda, Brad A. Grueter, and Laura L. Dugan.

Robust Expression of Functional NMDA Receptors in Human iPSC-Derived Neuronal Cultures Using an Accelerated Protocol

4.1 Introduction

N-methyl-D-aspartate (NMDA) receptors are ionotropic glutamatergic receptors which are critical for neurotransmission and higher-order function of the nervous system, including long-term potentiation (LTP), memory formation and consolidation, and maintenance of neuronal plasticity [196-200]. Activation of NMDA receptors (NMDARs) requires both the receptor ligand, glutamate, and a depolarizing stimulus to release Mg^{2+} inhibition of the receptor, and thus are often referred to as "coincidence detectors" [197, 199]. One defining hallmark of NMDAR activation is flux of Ca^{2+} through the ion channel to produce local increases in intracellular Ca^{2+}, and subsequent activation of calcium-dependent signaling pathways [197-199].

Much of our understanding of NMDAR function has come from studies on cell cultures from rodents and other non-primate animal model systems, or from immortalized cell lines with induced expression of human NMDAR subunits. However, emerging evidence suggests that there are important genetic, molecular, and functional differences between NMDARs in primates, including humans, and other species, specifically rodents, which may modify NMDAR composition, activation, and downstream signaling. For example,

differences between mice and humans in protein abundance of postsynaptic density factors found in the NMDAR complex have been reported [201]. These differences could have major implications for understanding the roles of NMDARs in health and disease and as drug targets. Thus, the ability to study human NMDARs in the context of all the regulatory and co-activating factors necessary for human neuronal function may be critical to understanding the roles of NMDARs in physiologic and pathophysiologic conditions.

Human neurons grown from induced pluripotent stem cells (iPSCs) provide an excellent opportunity to study human NMDARs in health and disease. However, only a limited number of published protocols have documented maturation of NMDARs molecularly or reported Ca^{2+} influx attributed to functional NMDARs; these protocols have limitations, including culturing cells for long periods of time [202-205], co-culturing with rodent astrocytes [80, 206], or culturing 3-D organoids [207-210] which are challenging to image [211-213].

Additionally, the glutamate-dependent currents that were identified via electrophysiology in many of the protocols cited above could have been evoked by either sodium or calcium. Sodium influx through NMDARs is likely dramatically greater than calcium influx, as NMDAR activation produces intracellular sodium increases in the millimolar range and intracellular calcium increases in the nanomolar range [214]. In contrast, calcium imaging exclusively identifies calcium flux through NMDARs.

Our interest in NMDARs in nervous system disease led us to develop an accelerated protocol to produce robust monolayer cultures with functional human NMDARs. The cultures demonstrate increased intracellular Ca^{2+} in response to NMDA and exhibit NMDAR-mediated electrically evoked postsynaptic current. Our procedure starts with

iPSC-derived neural progenitor cells (NPCs; defined as SOX1- and Nestin-positive cells). We successfully converted 3 separate iPSC-derived NPC lines to mature, fully functional neurons with our protocol.

4.2 Method

4.2.1 Reagents and Antibodies

6-well cell culture plates, Matrigel, and Laminin were purchased from Corning. Poly-L-ornithine hydrobromide (PLO), cAMP, L-Ascorbic Acid, paraformaldehyde, dimethyl sulfoxide, and RIPA Buffer were purchased from Sigma. DMEM/F12, B-27 Supplement, and GlutaMAX Supplement were purchased from Gibco. 35 mm glass bottom dishes were purchased from MatTek. TRIzol Reagent and Fluo-4, AM were purchased from Invitrogen. OneStep RT-PCR Kit was purchased from Qiagen. Primers were purchased from Integrated DNA Technologies. cOmplete, Mini Protease Inhibitor Cocktail was purchased from Roche. Pierce BCA Protein Assay Kit and SuperSignal West Femto Maximum Sensitivity Substrate were purchased from Thermo Scientific.

NMDAR1, NMDAR2A, MAP2, and GFAP antibodies were purchased from abcam (Cambridge, MA). TUJ1 antibody was purchased from Neuromics (Edina, MN). PSD95 antibody was purchased from Cell Signaling Technology (Danvers, MA). Synaptotagmin-1 antibody was purchased from Developmental Studies Hybridoma Bank (Iowa City, IA). NMDAR2B antibody was purchased from BD Transduction Laboratories (San Jose, CA). GFAP antibody was purchased from Calbiochem (Burlington, MA). All fluorescent secondary antibodies were purchased from Life Technologies (Waltham, MA). Mouse and rat HRP secondary antibodies were purchased from Invitrogen (Waltham, MA).

4.2.2 Cell Culture

A cryopreserved human NPC line derived from female human iPSCs (XCL-4; STEMCELL Technologies, Vancouver, 70902) was obtained. These NPCs are provided as greater than or equal to 90% SOX1-positive and Nestin-positive cells. The XCL-4 line was expanded in Neural Progenitor Medium 2 (STEMCELL Technologies, 08560) or in NSC Maintenance Medium with Supplements A and B (XCell Science, Novato, CA, SM-001-BM100, SM-001-SA100, and SM-001-SB100) on 6-well cell culture plates (Corning, 353846) coated with Matrigel (Corning, 354277). Neural Progenitor Medium 2 was discontinued, which necessitated the media switch. After three passages, cells were plated on 6-well plates coated with 15 µg/mL PLO (Sigma, P3655) and 10 µg/mL Laminin (Corning, 354232) at a plating density of $5X10^4$ cells per cm^2. Cells were fed every day with STEMdiff Neuron Differentiation medium (STEMCELL Technologies, 08500) or STEMdiff Forebrain Neuron Differentiation medium (STEMCELL Technologies, 08600) for 6-7 days until cells were 90-95% confluent. STEMdiff Neuron Differentiation medium was discontinued, which necessitated the media switch. Cells were treated with ACCUTASE Cell detachment solution (STEMCELL Technologies, 07920) for 5-10 minutes, washed with DMEM/F12 (Gibco, 11330-032) and pelleted by centrifugation at 1500 x g for 5 minutes at room temperature. Cells were resuspended in STEMdiff Neuron Maturation medium (STEMCELL Technologies, 08510) or STEMdiff Forebrain Neuron Maturation medium (STEMCELL Technologies, 08605) and were plated onto either 35 mm glass bottom dishes (for confocal imaging; MatTek, P35G-1.5-14-C) or 6-well plates (for Western blot and RT-PCR) coated with PLO/Laminin at a plating density of $2.5\text{-}5X10^5$ cells per dish or well. STEMdiff Neuron Maturation medium was discontinued, which necessitated the media switch.

In one experiment, cells were fed every other day with STEMdiff Neuron Maturation medium for the entire maturation period. For all other experiments, cells were fed every other day with STEMdiff Neuron Maturation medium or STEMdiff Forebrain Neuron Maturation medium for 7 days and then were fed every other day with Neurobasal Medium (Gibco, 21103-049) or (for cultures after STEMdiff Neuron Differentiation medium and STEMdiff Neuron Maturation medium were discontinued) BrainPhys Neuronal Medium (STEMCELL Technologies, 05790) supplemented with B-27 Supplement (Gibco, 17504-044) or NeuroCult SM1 Neuronal Supplement (STEMCELL Technologies, 05711), GlutaMAX Supplement (Gibco, 35050-061), 20 ng/mL BDNF (STEMCELL Technologies, 78005), 0.5 mM cAMP (Sigma, D0627), 0.2 mM L-Ascorbic acid (Sigma, A8960), and 10 µg/mL Laminin. Cells were in maturation media for 25-45 days.

4.2.3 RT-PCR

Total RNA was isolated by adding TRIzol Reagent (Invitrogen, 15596026) to each well, and RNA extraction was performed according to the manufacturer's protocol. Total RNA concentration was measured using a NanoDrop. 0.5 µg of RNA was used to generate cDNA, and the QIAGEN OneStep RT-PCR Kit (210212) was used to amplify the cDNA. A final volume of 25 µL per PCR reaction was used. We used the GluN1, GluN2A, GluN2B, GluN2C, GluN2D, GluN3A, and GluN3B human target cDNA primers listed in [215], and, as a control, the GAPDH primer listed in [123] to measure RNA expression. The final product was detected using a 2% agarose gel with ethidium bromide.

4.2.4 Western Blot

Cells were rinsed twice with PBS and were scraped in PBS before being pelleted by refrigerated centrifugation. The supernatant was discarded, and cell pellets were resuspended in RIPA Buffer (Sigma, R2078) containing 1% SDS and cOmplete, Mini Protease Inhibitor Cocktail (Roche, 4693124001). Cells were lysed by sonication on ice (https://www.abcam.com/ps/products/133/ab133625/documents/Lysate%20Preparation%20Protocol%20v3%20(website).pdf). Note that supernatant and particulate were not separated. Protein concentration was measured using the Pierce BCA Protein Assay Kit (Thermo Scientific, 23225). Total cell lysates were stored at -80°C. 10% SDS-PAGE gels were used. Gels were transferred overnight at 4°C onto PVDF membranes. Membranes were blocked in 5% milk in PBST for one hour and incubated overnight with NMDAR1 (abcam, ab109182, RRID:AB_10862307, 1:1000 dilution), NMDAR2A (abcam, ab124913, RRID:AB_10975154, 1:1000 dilution), NMDAR2B (BD Transduction Laboratories, 610417, RRID:AB_397797, 1:500 dilution), and GAPDH (Invitrogen, MA5-15738, RRID:AB_10977387, 1:5000 dilution) primary antibodies in 5% milk in PBST. Membranes were washed three times with PBST, incubated in corresponding HRP secondary antibodies in PBST for one hour at room temperature, and washed three times with PBST before visualizing using SuperSignal West Femto Maximum Sensitivity Substrate (Thermo Scientific, 34095) according to the manufacturer's protocol using a G:BOX and the associated GeneSys software (Syngene, RRID:SCR_015770).

4.2.5 Immunohistochemistry

Cells cultured on 35 mm glass bottom dishes were fixed with 4% paraformaldehyde

(Sigma, 158127) for 15-30 minutes and then washed 2-3 times with PBS. Cells were permeabilized with 2% BSA and 0.3% Triton X-100 for 30 minutes. Cells were washed twice with PBS containing 2% BSA and were incubated with TUJ1 (Neuromics, CH23005, RRID:AB_2210684, 1:2000 dilution; or BioLegend, 801202, RRID:AB_10063408, 1:1000 dilution), MAP2 (abcam; ab32454, RRID:AB_776174, 1:2000 dilution), NMDAR1 (BioLegend, 818601, RRID:AB_2564822, 1:400 dilution), NMDAR2A (Millipore, AB1555P, RRID:AB_90770, 1:200 dilution), NMDAR2B (Millipore, AB1557P, RRID:AB_90772, 1:200 dilution), PSD95 (Cell Signaling Technology, 3450, RRID:AB_2292883, 1:200 dilution), synaptotagmin-1 (Developmental Studies Hybridoma Bank, mAB 30, RRID:AB_2295002, 1:200 dilution), and/or GFAP (Calbiochem, 345860, RRID:AB_2109651, 1:2000 dilution) primary antibodies in PBS containing 2% BSA overnight. Cells were washed twice with PBS containing 2% BSA, were incubated with corresponding fluorescent secondary antibodies for one hour at room temperature, and then washed 3 times with PBS and treated with DAPI before imaging on an LSM 880/Axio Observer.Z1 confocal microscope (Zeiss). Images were processed in Fiji (RRID:SCR_002285).

4.2.6 Calcium Imaging

One vial of Fluo-4, AM (Invitrogen, F14201) was dissolved in 50 µL of dimethyl sulfoxide (Sigma, D2650) before being added to 10 mL of HEPES-bicarbonate balanced salt solution with 5.5 mM D-glucose ($HBBSS_{5.5}$) [216]. Cells cultured on 35 mm glass bottom dishes were incubated with Fluo-4, AM in $HBBSS_{5.5}$ for 30 minutes in the CO_2 incubator before being washed once with 1 mL of $HBBSS_{5.5}$. When ready to image on an LSM 880/Axio Observer.Z1 confocal microscope (Zeiss), 10 µL of 10 mM glycine (final concentration:

100 µM; RPI, G36050) was added to the dish for 5 minutes at room temperature. Time series imaging was performed with an interval of 1-3 minutes per image. Two baseline images were taken prior to the addition of 100 µL of vehicle ($HBBSS_{5.5}$) or 0.5-3 mM NMDA (final concentration: 50-300 µM; Sigma, M3262). In some cultures, 100 µL of 100 µM of the NMDAR antagonist MK-801 (final concentration: 10 µM; Sigma, M107) was added after additional images were taken.

4.2.7 Calcium Imaging Analysis

For each calcium imaging experiment, using MetaMorph (Molecular Devices, RRID:SCR_002368), brightness was artificially increased and individual cells (identified by presence of Fluo-4) in the first image were circled. Brightness was then reset to normal and Fluo-4 fluorescence intensity was logged for every cell for each image of the experiment. Intensity values for the first two images of every cell were averaged, with this value being considered the baseline fluorescence intensity. Data was normalized to this baseline.

4.2.8 Electrophysiology

Whole-cell voltage clamp recordings were performed on XCL-4 derived mature cultures (37-39 days in maturation media) transferred into artificial cerebral spinal fluid (in mM: 119 NaCl, 2.5 KCl, 1.3 $MgCl_2$-$6H_2O$, 2.5 $CaCl_2$-$2H_2O$, 1.0 NaH_2PO_4-H_2O, 26.2 $NaHCO_3$, and 11 glucose; 290-295 mOsm) and patched with 4–6 MΩ recording pipettes (pulled with a P-1000 Micropipette Puller; Sutter Instrument) using a Cs^+-based intracellular solution (in mM: 120 $CsMeSO_3$, 15 CsCl, 8 NaCl, 10 HEPES, 0.2 EGTA, 10 TEA-Cl, 4.0 Mg-

ATP, 0.3 Na-GTP, 0.1 spermine, and 5.0 QX 314 bromide; 290 mOsm). NMDAR-mediated electrically evoked excitatory postsynaptic currents were obtained at +40 mV using a parallel bipolar electrode (FHC Worldwide, customized 30210-PBSA1045) and isolated with the $GABA_A$ receptor antagonist, picrotoxin (final concentration: 50 µM; Sigma), and the AMPA receptor antagonist, NBQX (final concentration: 5 µM; Tocris Bioscience), and were then blocked using the NMDAR antagonist, AP5 (final concentration: 50 µM; Tocris Bioscience). Inclusion criteria for cells were a steady (< 20% change) access resistance (R_A) of < 16 mΩs, and a steady holding current of < -100 pA at -70 mV.

4.2.9 Statistical Analysis

All statistics were performed using SigmaPlot 14.5 (Inpixon, Palo Alto, CA, RRID:SCR_003210). One-way analysis of variance (ANOVA) and Holm-Sidak tests were performed for Figure 4.7C. One-way repeated measures ANOVA and Bonferroni tests were performed for Figure 4.8D. Significant differences were noted if $p < 0.05$.

4.3 Results

4.3.1 Development and Maturation of iPSC-Derived Neuronal Cultures

We chose to establish a protocol which utilized NPCs derived from human iPSCs (Figure 4.1). Three lines were used (Figures 4.2 and 4.3). Immunohistochemistry of XCL-4 converted mature cell cultures exhibited the presence of β-tubulin III (Figures 4.4A,B), microtubule-associated protein 2 (Figures 4.4A,D), NMDAR1 (Figures 4.4B and 4.5), NMDAR2A (Figure 4.5), NMDAR2B (Figure 4.5), synaptotagmin 1 (Figure 4.4C), and

postsynaptic density protein 95 (Figure 4.4C), which are markers indicative of mature neurons. GFAP-positive astrocytes (Figure 4.4D) are also present in the same converted cultures. We observed that the cultures contain approximately 20-30% astrocytes (based on counts of DAPI and GFAP from 4 different fields of the same dish).

4.3.2 Developmental Expression of Markers of Mature NMDARs

Mature XCL-4 derived neurons were harvested at various maturation days to determine NMDAR subunit expression by RT-PCR (Figures 4.6A-D) and by Western blot (Figure 4.6E).

4.3.3 Presence of Functional NMDARs in the Mature Cultures

To confirm that the NMDARs in the XCL-4 converted cultures are functional, we performed Fluo-4 fluorescent calcium imaging and found that NMDA treatment enhances calcium signaling in the cultures (Figures 4.7A-C and 4.8B-D), while treatment with an NMDAR antagonist inhibits calcium signaling (Figures 4.8C,D). Vehicle treatment has no effect on calcium signaling (Figures 4.7A-C and 4.8A). To validate that the NMDARs in our cultures are functional at the synapse, we performed whole-cell voltage clamp electrophysiology. In the presence of $GABA_A$ receptor and AMPA receptor antagonists, electrical stimulation elicited a postsynaptic current (mean peak = 16.99 pA, SD = 8.96 pA, n = 7 cells) sensitive to an NMDAR antagonist (Figure 4.8E).

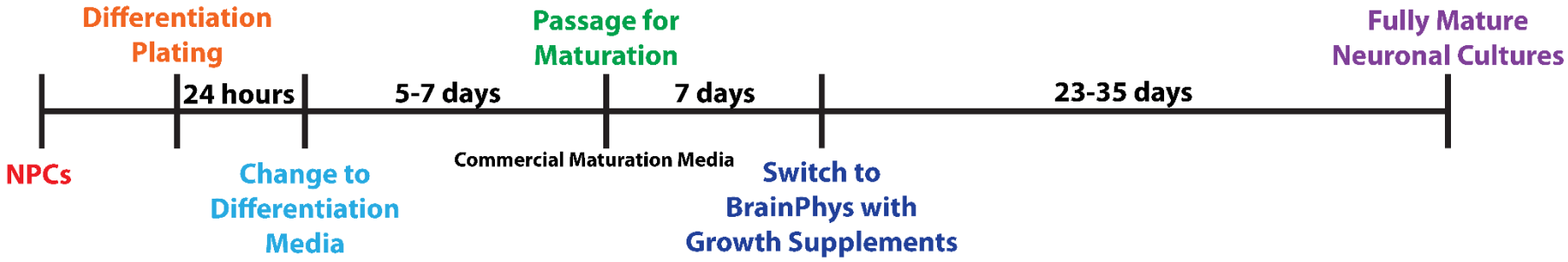

Figure 4.1. Protocol sequence for differentiation and maturation of human neuronal cultures. Cryopreserved vials of NPC lines were maintained in liquid nitrogen until use. After thawing, cells were plated for differentiation. Cells were transitioned through each step as depicted in this figure and as described in detail in Method.

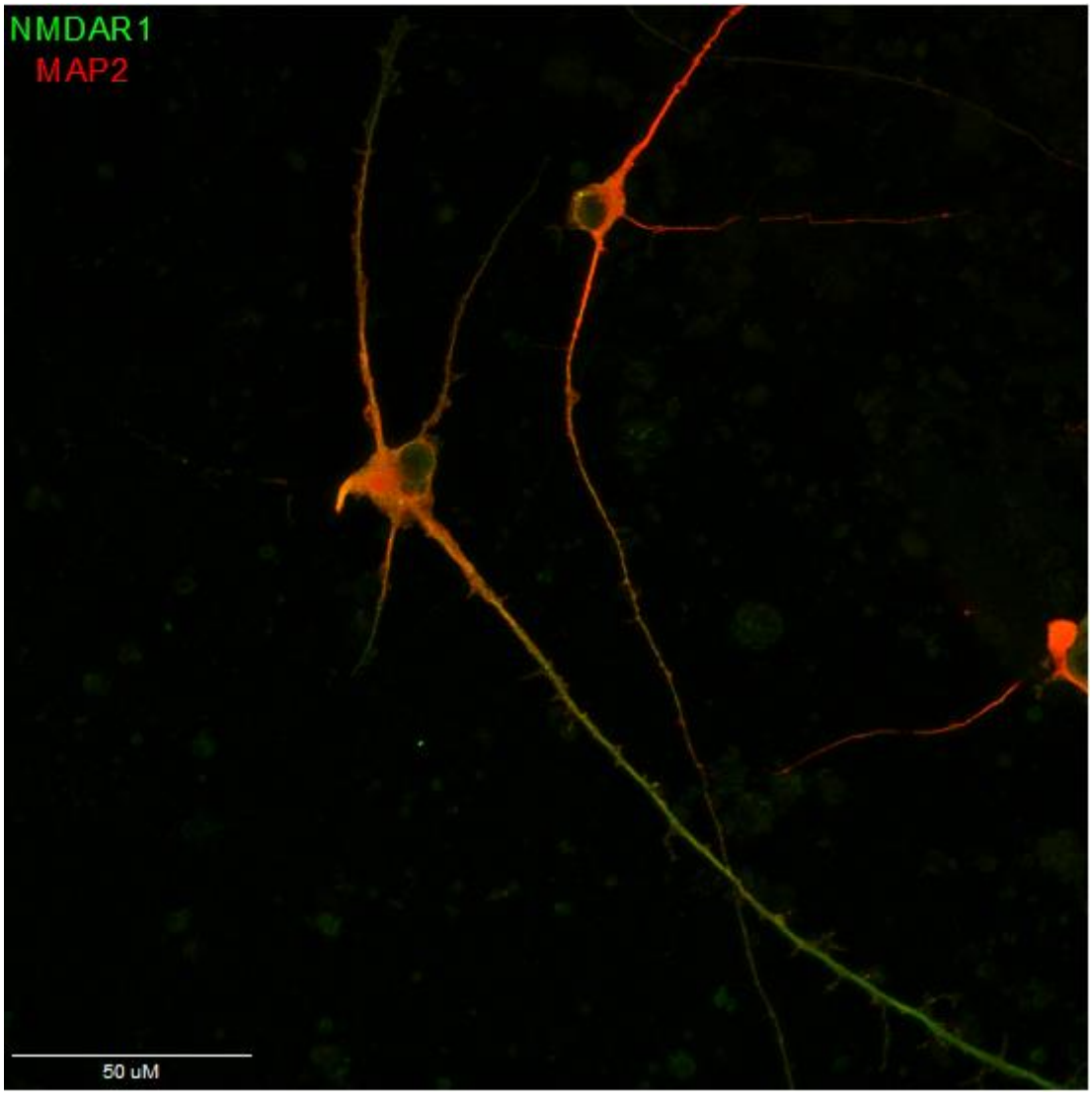

Figure 4.2. Immunofluorescent confocal imaging of mature iPSC-derived neuronal cultures. Using a well-established control female human iPSC line, CC3 [217], and an earlier iteration of the protocol described in the main text, cells were converted into mature neurons and were fixed, permeabilized, and stained for the mature excitatory neuron markers MAP2 (red) and NMDAR1 (green). Cultures also exhibited extensive arborization of both axons and dendrites.

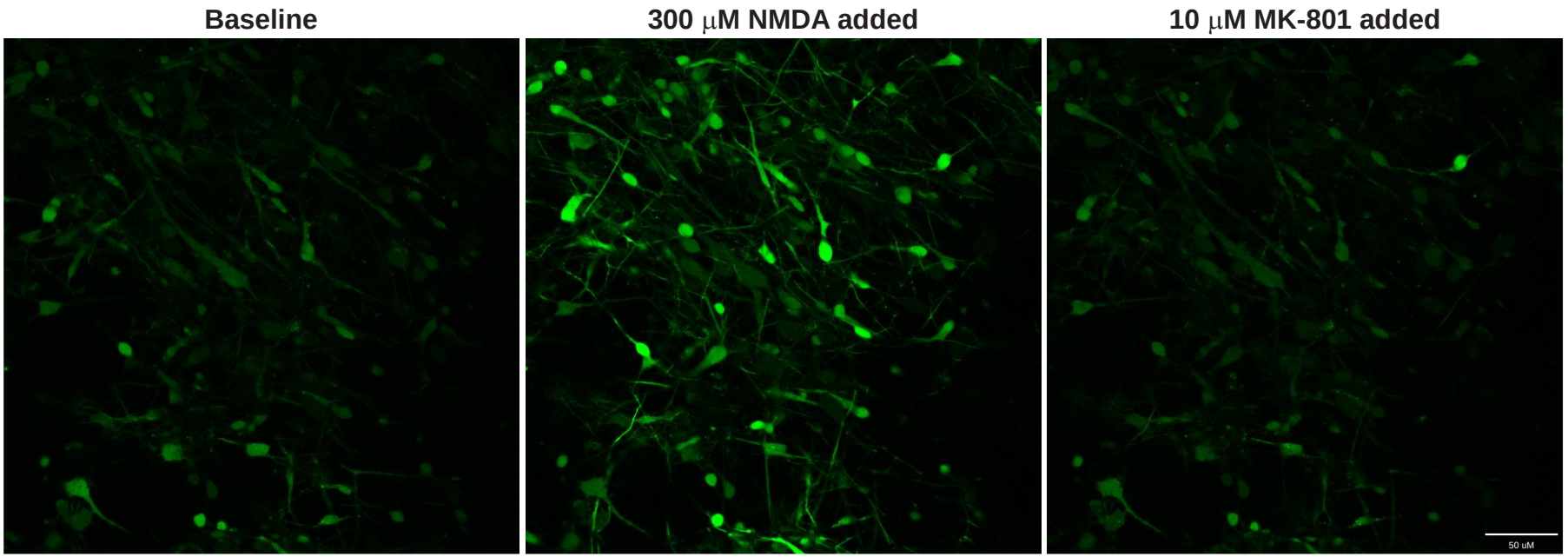

Figure 4.3. Mature patient iPSC-derived neuronal cultures express functional NMDA receptors. Mature cultures (37 days in maturation media) derived from the BV3525A#1 female human iPSC line were loaded with the calcium indicator Fluo-4 for 30 minutes and then washed with $HBBSS_{5.5}$ media, followed by the addition of glycine (final concentration of 100 µM) prior to imaging. Using a time series protocol at 40X magnification, two baseline images were taken prior to the addition of a final concentration of 300 µM NMDA. The NMDAR antagonist MK-801 at a final concentration of 10 µM was added after additional images were taken. Images at baseline, after addition of NMDA, and after addition of MK-801, are shown.

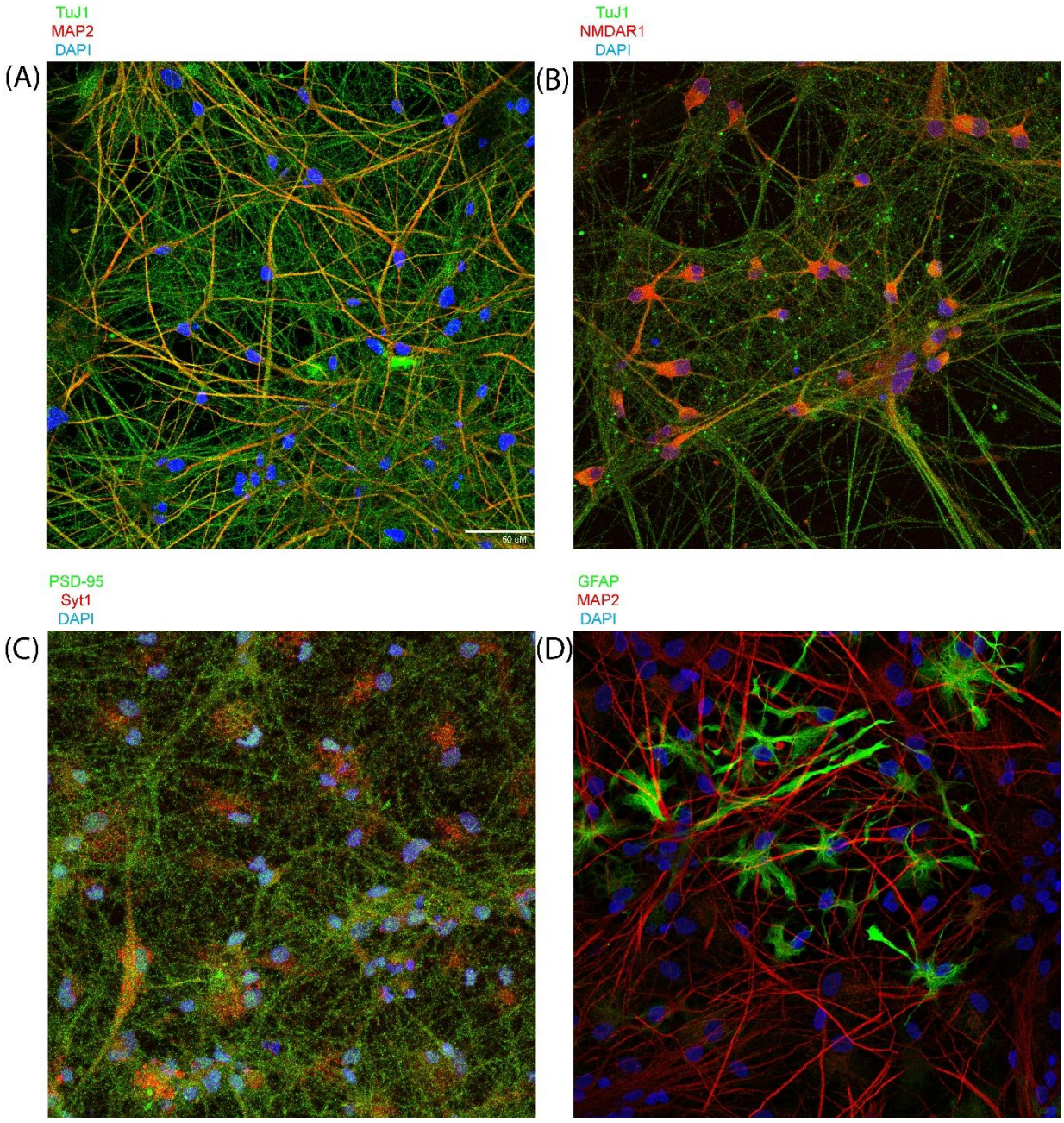

Figure 4.4. Immunofluorescent confocal imaging and characterization of mature human neuronal cultures. **(A-D)** XCL-4 derived mature cultures (28-37 days in maturation media) were fixed, permeabilized, and stained for the mature excitatory neuron markers β-tubulin III (TuJ1; green; A-B) and microtubule-associated protein 2 (MAP2; red; A,D), the obligate NMDAR subunit, NMDAR1 (red; B), the presynaptic marker synaptotagmin 1 (Syt1; red; C), the postsynaptic marker postsynaptic density protein 95 (PSD-95; green; C), and the astrocytic marker glial fibrillary acidic protein (GFAP; green; D). All cultures were counterstained with the nuclear stain DAPI (blue; A-D).

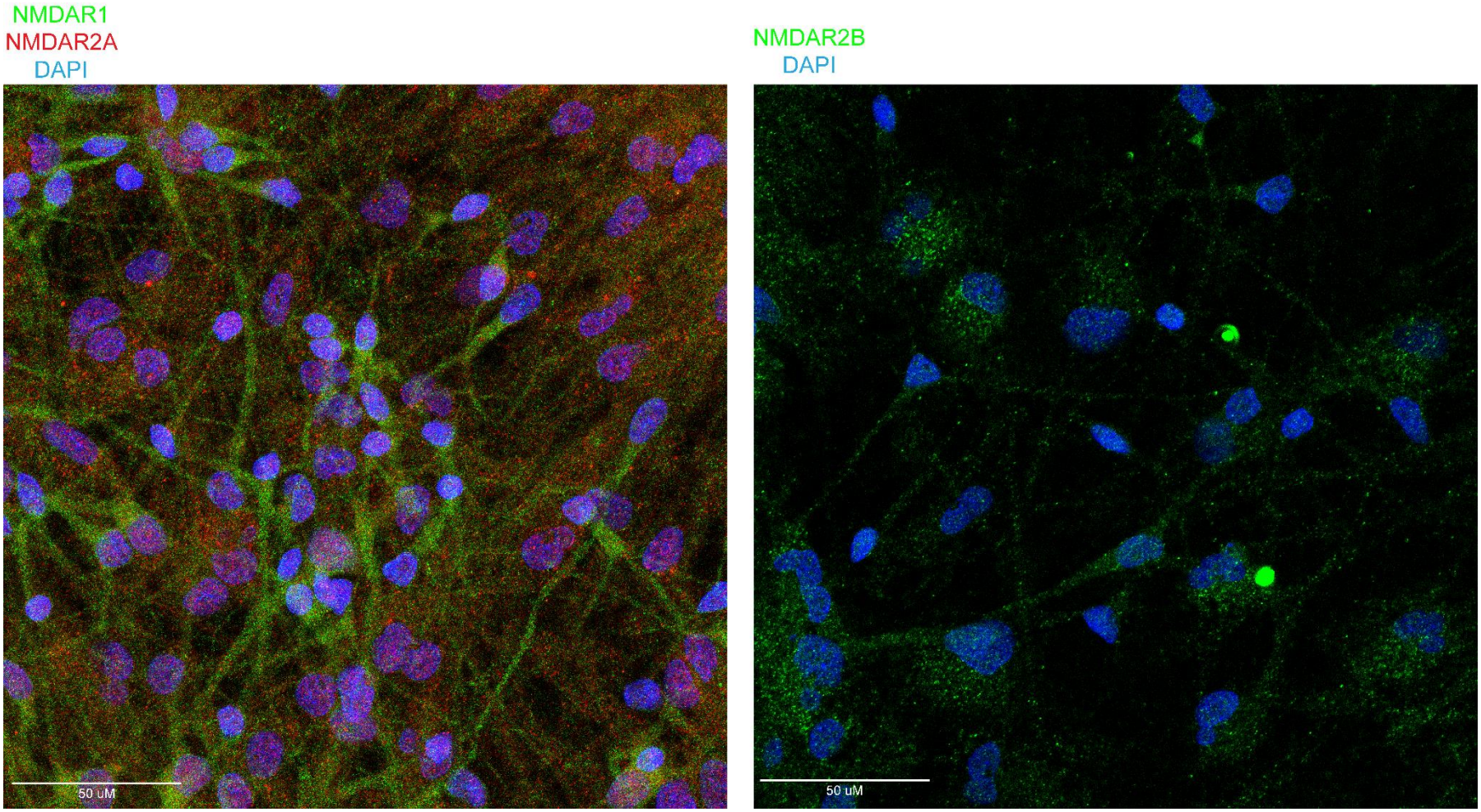

Figure 4.5. Immunofluorescent confocal imaging of NMDA receptor subunits in mature human neuronal cultures. XCL-4 derived mature cultures (37 days in maturation media) were fixed, permeabilized, and stained for NMDAR1 and NMDAR2A (green and red, respectively; left) and NMDAR2B (green; right), and counterstained with the nuclear stain DAPI (blue).

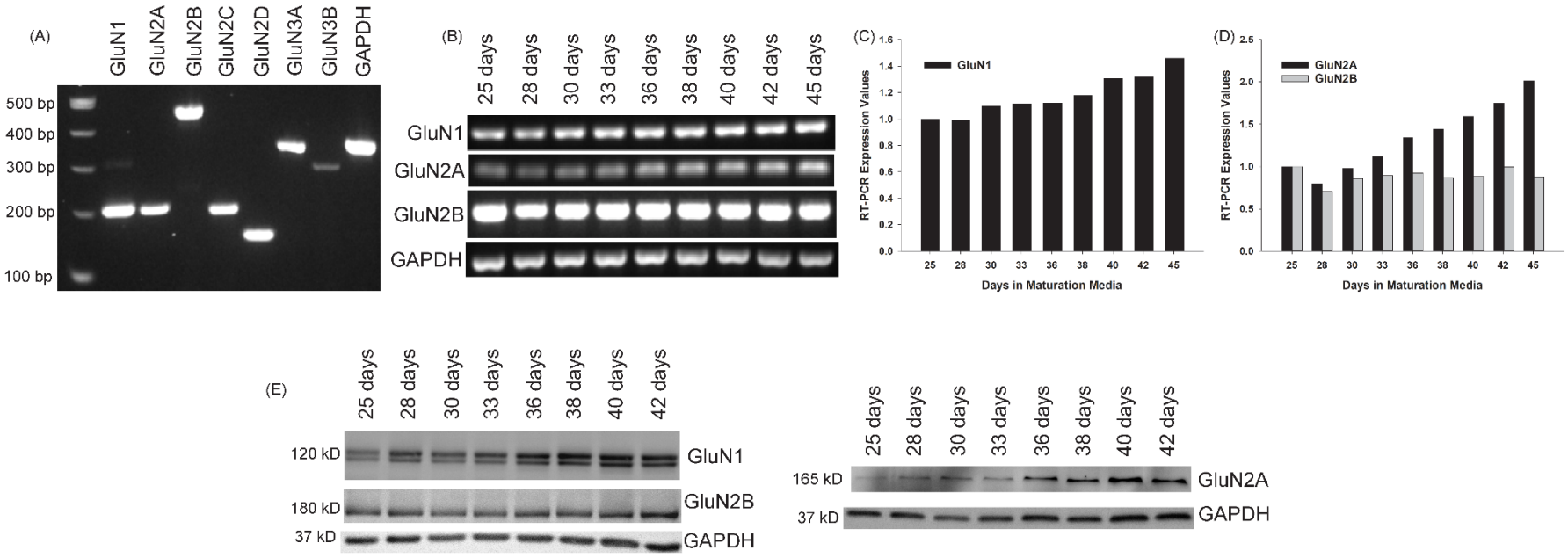

Figure 4.6. Expression of NMDAR subunits in maturing human neuronal cultures. **(A)** RT-PCR was performed with RNA harvested from XCL-4 derived mature neuronal cultures (36 days in maturation media) to confirm the expression of several of the NMDAR subunits. **(B-D)** A time course study was performed with RNA harvested from cultures in maturation media at increasing times starting at 25 days to assess NMDAR subunit expression (B) and displayed quantitatively (C-D). **(E)** NMDAR subunit protein expression was assessed by Western immunoblot at various stages of culture maturation.

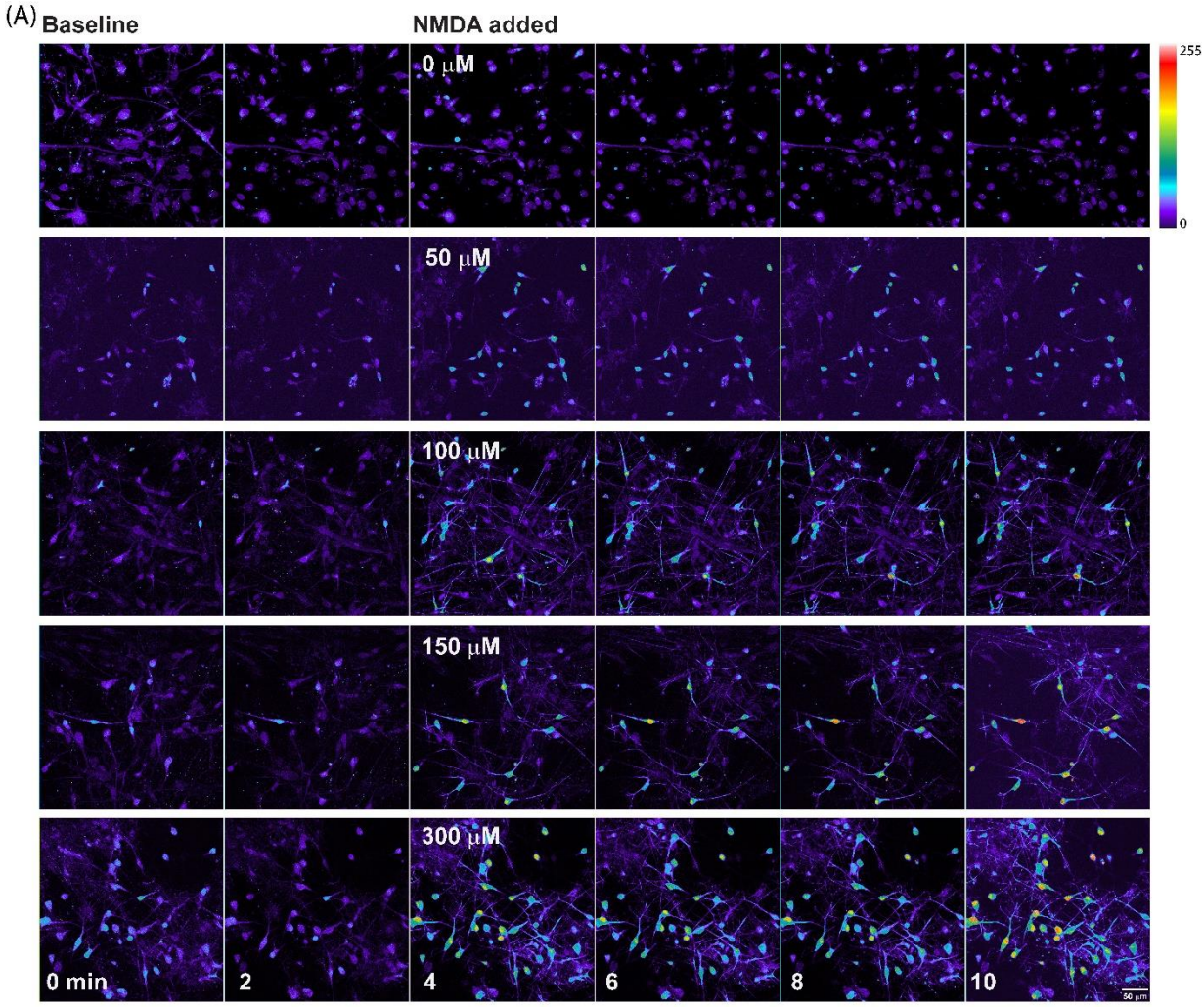
(A)
Baseline
NMDA added
0 μM
50 μM
100 μM
150 μM
300 μM
255
0
0 min
2
4
6
8
10
(B)
Fluo-4 Fluorescence Intensity
Time (minutes)
0
50
100
150
300
(C)
n.s.
***
*
*
Fluo-4 Fluorescence Intensity
NMDA (μM)

Figure 4.7. Confocal imaging of intracellular calcium in human neurons exposed to NMDA. XCL-4 derived mature cultures (41-42 days in maturation media) were loaded with the calcium indicator Fluo-4 for 30 minutes and then washed with $HBBSS_{5.5}$ media, followed by the addition of glycine (final concentration of 100 µM) prior to imaging. Using a time series protocol at 40X magnification, images were taken every two minutes. Two baseline images were taken prior to the addition of vehicle ($HBBSS_{5.5}$), or increasing final concentrations of NMDA by bath application, and then four additional images were taken. **(A)** NMDA dose-response montages are shown. Images were converted to a linear pseudocolor scale using MetaMorph. Individual cells were identified and Fluo-4 fluorescence intensity at each time point was measured. The intensity of cells at each time point were averaged together. **(B-C)** Data were graphed using SigmaPlot 12 (full time series from one experiment, B; ten-minute time point from 5 independent replicates, C) and one-way analysis of variance (ANOVA) and Holm-Sidak tests were performed for (C) using SigmaPlot 14.5. Data are represented as mean + SEM. ***$P < 0.001$; *$P < 0.05$; n.s. = not significant. n = 32-74 cells per condition.

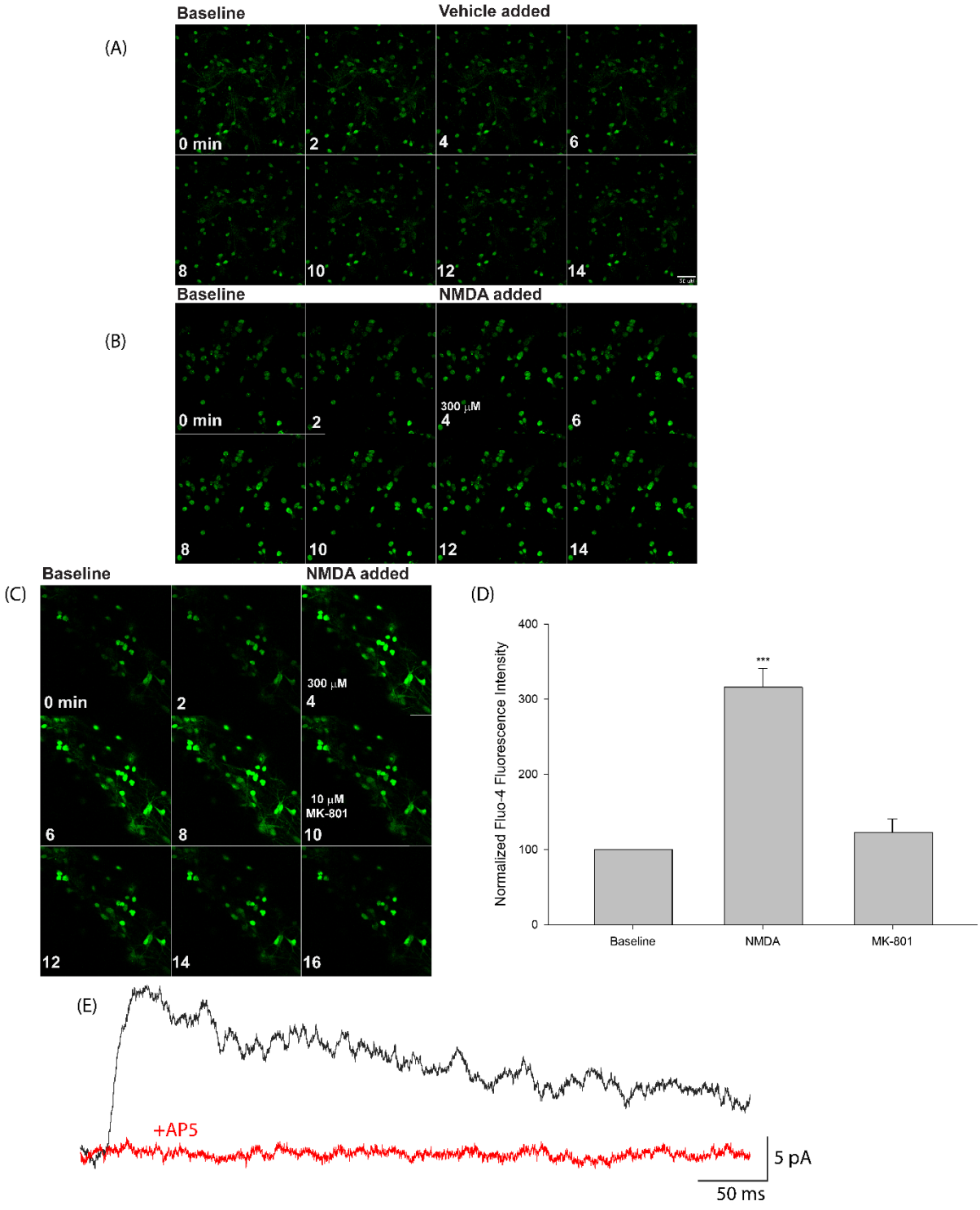
(A)
Baseline
Vehicle added
0 min
2
4
6
8
10
12
14
(B)
Baseline
NMDA added
0 min
2
300 µM
4
6
8
10
12
14
(C)
Baseline
NMDA added
0 min
2
300 µM
4
6
8
10 µM
MK-801
10
12
14
16
(D)
Normalized Fluo-4 Fluorescence Intensity
400
300
200
100
0
***
Baseline
NMDA
MK-801
(E)
+AP5
5 pA
50 ms

Figure 4.8. Mature iPSC-derived neuronal cultures express functional NMDA receptors. XCL-4 derived mature cultures (30-39 days in maturation media) were loaded with the calcium indicator Fluo-4 for 30 minutes and then washed with $HBBSS_{5.5}$ media, followed by the addition of glycine (final concentration of 100 µM) prior to imaging. Using a time series protocol at 40X magnification, two baseline images were taken prior to the addition of vehicle ($HBBSS_{5.5}$), or a final concentration of 300 µM NMDA. For some cultures, the NMDAR antagonist MK-801 at a final concentration of 10 µM was added after additional images were taken. **(A-C)** Representative montages are shown. Fluo-4 time series images were analyzed using MetaMorph. Individual cells were identified and Fluo-4 fluorescence intensity at each time point was measured. The intensity of cells at each time point were averaged together. The first two time points were averaged as the baseline intensity, and all data were normalized to the corresponding baseline. **(D)** Data from the montage shown in (C) were graphed using SigmaPlot 14.5. One-way repeated measures ANOVA and Bonferroni tests were performed using SigmaPlot 14.5. Data are represented as mean + SEM. ***$P < 0.001$. n = 21 cells per condition. **(E)** A representative trace is shown of an NMDAR-mediated electrically evoked postsynaptic current from XCL-4 derived mature cells in the presence of the $GABA_A$ receptor antagonist, picrotoxin (final concentration: 50 µM), and the AMPA receptor antagonist, NBQX (final concentration: 5 µM), before (black) and after (red) application of the NMDAR antagonist, AP5 (final concentration: 50 µM).

4.4 Discussion

Experiments utilizing neurons derived from human iPSCs are critical to ultimately treat and prevent human disease, as there are many important differences between human and rodent neurons, including regarding their NMDARs. For example, a primate-specific short isoform of the NMDAR 2A subunit (GluN2A-S) was recently identified which can co-assemble to form a functional NMDAR, but whose function has not yet been defined [31]. Additionally, while the GluN2B to GluN2A developmental switch is evolutionarily conserved [200], this switch occurs earlier in humans than in rodents [218]. Also, GluN2A and GluN2C subunits are present before birth in humans but not in rodents [219, 220]. Sequence identity between rat and human GluN2C subunits is only 87.1%, and the sequence identity of the carboxy-terminal domains between rat and human GluN2C subunits is only 71%, suggesting that differences in membrane trafficking and phosphorylation may exist [221]. Two GluN2C/D selective modulators were found to be less potent for rat GluN2C-containing receptors compared to human GluN2C-containing receptors [221].

Our protocol yields forebrain-type neurons, like other protocols [222-224]. The vast majority of neurons are excitatory. Our protocol generates mature neurons in only 37 days (approximately 5 weeks), while other protocols culture cells for 7 to 12 weeks or longer before mature neurons are generated [202-205]. Additionally, our XCL-4 converted cultures contain both neurons and astrocytes derived from the same human cell line. Astrocytes are an important nervous system component, as they are closely associated with and can alter the function of synapses [225, 226]. The absence of astrocytes from other species in our cultures, unlike other protocols that co-culture with rodent astrocytes [80, 206], is noteworthy, as there are other key differences between human and animal model

systems that are crucial to understand age-related effects on brain. Inflammation and activation of innate immunity are believed to underlie much of aging biology. However, humans express several inflammatory mediators that are not present in rodents. For example, NADPH oxidase 5 (NOX5), which is calcium-dependent, is expressed in primates, but not rodents or lower organisms [227]. NOX5's expression in human neurons, and responsiveness to calcium to induce free radical production, could contribute importantly to inflammation in the brain, yet is most likely to be studied effectively only in human (or other primate) cells. Thus, there is a pressing need for models which retain the features unique to humans to allow for accurate characterization of human NMDARs in both physiologic and pathophysiologic conditions.

Our protocol begins with cell lines at the NPC stage. The rationale for starting with NPCs is several-fold. There are multiple published procedures for conversion of iPSCs to NPCs [228]. Working with NPCs as the starting lineage allows quick expansion of the NPC line from frozen aliquots, and, importantly, many institutions have turned to core facilities to perform the initial collection of patient tissue, conversion to iPSCs, and differentiation to tissue-specific precursor stem cell lines, with these cell lines provided to the end-user. This is because of the increased patient protection and consenting requirements for iPSC generation and specialized requirements for iPSC viral transformation that are difficult for individual labs to provide [229-231].

We utilized calcium imaging and electrophysiology to confirm that the NMDARs in our cultures were functional. Studying calcium dynamics on the order of minutes allows enough time for the addition of multiple substrates (such as NMDA and then MK-801) to the neuronal cultures being imaged. Studying slower calcium dynamics also does not require the elaborate and expensive setups used by those who study fast calcium dynamics.

Even though we found the expression of various NMDAR subunits at maturation day 28, calcium imaging performed at that time point did not show the presence of robust functional NMDARs (data not shown). Characterization of cultures derived from a new protocol must include functional assays such as calcium imaging and electrophysiology to fully assess the conditions of the cultures.

We also converted patient fibroblast (BV3525A#1 iPSC line) derived NPCs to neurons with functional NMDARs in a short period of time. Our current protocol provides a basis for future drug targeting and screening for neurological diseases in a considerably shorter time frame. Soon, we envision that a patient presenting with a disease where impaired NMDARs may be implicated can have their tissue samples collected. Patient-derived iPSCs will immediately be generated and converted into mature neurons within weeks for specific therapeutic testing. The results of this testing will impact the future treatment plan of that same patient. In the same way that many cancer treatments are now personalized, we hope that personalized treatments for neurological disorders can be similarly achieved.

CHAPTER 5

Discussion

5.1 Overview

Parvalbumin interneuron vulnerability has been the central theme of this dissertation. Chapter 2 provided background information about PV-INs, where injured PV-INs have been found, and why PV-INs may be so vulnerable. In Chapter 3, experiments where PV^{cre}-tdTomato mice were exposed to chronic hypoxia were described. PV-INs were found to be injured but not degenerated. In Chapter 4, human neurons with functional NMDA receptors were generated. PV-INs depend on the presence of functional NMDA receptors.

5.2 Relationship Between NMDA, Hypoxia, and PV-INs

The links between NMDA and hypoxia were not addressed in this dissertation, but there are many reports in the literature that explore the relationship between them. NMDA receptor responses in neonatal rat hippocampal neurons are suppressed by hypoxia, which may explain the innate hypoxia tolerance of mammalian neonates [232]. Induction of hypoxia in piglets led to increased NMDA receptor-mediated calcium influx and increased nitration of NMDA receptor subunits [233]. Short-term hypoxia reduced NMDA receptor magnesium block and induced long-term potentiation of NMDA transmission in a rat *in vitro* model of the retinocollicular pathway [234]. Intermittent hypoxia prevented NMDA receptor-dependent long-term potentiation and resulted in decreased expression of the NMDA receptor 1 subunit protein in mouse hippocampus [235]. These findings are just a sampling of what is known thus far about the interactions between hypoxia and NMDA.

There are also potential interactions between hypoxia, the NMDA receptor subunit GluN2A, and PV-INs. In the hypoxic brain, it is likely that GluN2A is oxidized, reducing the duration and likelihood of NMDA receptor channel opening and resulting in reduced calcium permeability [236-238]. Since GluN2A-containing NMDA receptor activity is crucial for proper functioning of PV-INs and for the preservation of parvalbumin immunoreactivity, as discussed in Chapter 2, hypoxia could be injuring PV-INs in part through oxidation of GluN2A. If a return to normoxia occurs too quickly, GluN2A would be reduced, resulting in a rapid influx of calcium into PV-INs. Since the hypoxic exposure has already damaged parvalbumin protein, the influx of calcium could further injure PV-INs, as schematized in Figure 2.1B.

5.3 Unanswered Questions

What is the mechanism of the PV-IN injury described in Chapter 3? Since IL-6 was increased in the mice exposed to chronic hypoxia, this could be similar to the mechanism described in Chapter 2 for PV-INs injured by ketamine, where IL-6-mediated Nox2-dependent NADPH oxidase is activated, and superoxide is produced. What is happening at the molecular level that accounts for the decreased parvalbumin immunoreactivity observed in Chapter 3? Changes to *Pvalb* gene expression, PVALB mRNA stability, and/or parvalbumin protein degradation could all potentially account for the decreased parvalbumin immunoreactivity. Future experiments could determine the mechanism of PV-IN injury and determine why parvalbumin immunoreactivity is decreased in the sustained hypoxia model.

Parvalbumin protein is likely regulated in part by calcium (see Chapter 2 for more about the

relationship between parvalbumin protein and calcium). What would happen to parvalbumin protein if NMDA receptors and calcium-permeable AMPA receptors on PV-INs were blocked, leading to a decrease in the amount of calcium entering the PV-INs? Depending on how long these receptors were blocked, this might result in a decrease in parvalbumin protein expression to compensate for the decreased need to buffer calcium. Then, if these receptors were suddenly unblocked, this could result in a rapid influx of calcium to PV-INs. Since there would no longer be enough parvalbumin protein present to bind this calcium, this could result in the pathological situation schematized in Figure 2.1B. However, if the receptors were gradually unblocked, there might be enough time for new parvalbumin protein to be synthesized, allowing for parvalbumin to successfully bind calcium entering the PV-INs.

What is happening at a physiological level to injured PV-INs with decreased amounts of parvalbumin protein? Network modeling suggests that a decrease in parvalbumin protein would result in an increase in asynchronous release of GABA, leading to decreased firing rates of PV-INs and a reduction in gamma band activity [107]. However, what is happening at a physiological level probably depends on whether the stressor leading to PV-IN injury is acute or chronic.

5.4 Future Directions

The experiments described in this dissertation provide a starting point for many further experiments that the Dugan Laboratory and, more broadly, the field should perform. The PV^{cre}-tdTomato mice described in Chapter 3 could be exposed to a wide array of pro-inflammatory insults, including ketamine and lipopolysaccharide [9, 25], to learn whether

the findings in Chapter 3 are pro-inflammatory insult-dependent or universal. If the sustained hypoxia model is somewhat unique in that parvalbumin interneurons degenerate in other pro-inflammatory models, then the conclusions and future directions from my chronic hypoxia experiments have limited application. If, however, parvalbumin interneurons are found not to degenerate in other pro-inflammatory models as well, then strategies to prevent and/or treat PV-IN injury could be broadly applied to almost any instance where PV-IN-related changes have been observed.

The PV^{cre}-tdTomato mice exposed to chronic hypoxia could be further characterized to observe whether other neuronal populations beyond PV-INs and calretinin interneurons are injured to better answer how uniquely vulnerable PV-INs are. The main reason that we did not look beyond these two populations is due to the time-intensive and labor-intensive nature of the image processing and analysis. If the tracing of neurons could be accomplished in an automated manner as opposed to the manual tracing that we performed, the model could be much more fully characterized within a reasonable amount of time. Additionally, automated tracing of neurons would remove the variability between experimenters who are tasked with deciding what "counts" as a neuron. I hope that automated neuron tracing will be available for laboratories around the world to make use of in the near future [239].

Additionally, mouse lines analogous to PV^{cre}-tdTomato mice, including CR^{cre}-tdTomato mice (crossing Ai9 mice with strain # 010774), CB^{cre}-tdTomato mice (crossing Ai9 mice with strain # 028532), and SST^{cre}-tdTomato mice (crossing Ai9 mice with strain # 013044), could be generated to be able to identify other neuronal populations irrespective of the level of immunostaining present for their namesake proteins. With the three lines mentioned above, we would learn whether injured but functional calretinin, calbindin, and somatostatin interneurons exist.

Since a subset of COVID-19 patients present with hypoxia, it was posited in Chapter 3 that PV-INs are likely injured in this subset of COVID-19 patients. Therefore, it would be of interest to assess PV-IN vulnerability via immunohistochemistry in the brains of those who died due to COVID-19, and of those who died sometime after recovering from COVID-19. If COVID-19 does result in PV-IN injury, there could be a difference in the degree of injury between those who died due to COVID-19 and those who died after having the disease at an earlier point in time. There could also be a difference between those who had Long COVID and those who did not, as some of the Long COVID CNS deficits could be due to PV-IN injury. If PV-INs are indeed injured in those with COVID-19, then strategies to treat PV-IN injury would be critically important for those who had COVID-19 and may be experiencing Long COVID symptoms.

PV-IN vulnerability could also be indirectly assessed in individuals with Long COVID CNS deficits who are still alive. Electroencephalography (EEG) can be used to measure gamma oscillations in individuals with Long COVID and individuals without the condition. If PV-INs are injured in individuals with Long COVID CNS deficits, then I would expect to see differences in gamma power and/or gamma oscillatory activity between groups, like what has been observed in schizophrenia (Table 2.1) and Alzheimer's disease (Table 2.2). If differences in gamma power and/or gamma oscillatory activity are observed between groups, then EEG could be utilized to determine whether experimental methods to treat Long COVID CNS deficits are rescuing PV-INs, as individuals being treated for Long COVID could be monitored longitudinally using EEG. If the treatment is rescuing PV-INs, then I would expect the gamma power and/or gamma oscillatory activity deficits to resolve.

We have modified the protocol described in Chapter 4 to enrich for PV-INs, which we accomplished by growing the cultures for a longer period of time and by supplementing the

feeding media with forskolin, a compound that stimulates adenylate cyclase to increase levels of cyclic AMP and that was suggested to increase the percentage of PV-INs by a prior publication [240]. The Dugan Laboratory is planning to treat PV-IN-enriched human neuronal cultures with pro-inflammatory stimuli. We want to determine how the treated PV-INs will respond to NMDA and to examine whether PV-INs treated with pro-inflammatory stimuli have decreased mean parvalbumin fluorescence per cell. The Dugan Laboratory has previously found that there is a decrease in mean parvalbumin fluorescence/cell in mouse primary neuronal cultures treated with the pro-inflammatory stimulus ketamine 24 hours prior to imaging [9], but it is not yet known whether human PV-INs will exhibit a similar response. As described in Chapters 1 and 4, there are key differences between rodent and primate neurons, so it is possible that results observed in a murine model could differ from results observed in a human model.

In Chapter 4, utilizing the NPC to neuron protocol to personalize treatments for neurological disorders was described. Now that we have modified the protocol to enrich for PV-INs, treatments for neurological disorders where PV-IN alterations are implicated could be even more personalized. We ultimately want to prevent or treat PV-IN injury to positively impact patients with diseases where PV-INs are known to be injured. The Dugan Laboratory has performed some initial experiments exploring how to prevent or treat PV-IN injury [9, 123, 124]. As mentioned in Chapter 2, GluN2A-selective NMDA receptor positive allosteric modulators should selectively target PV-INs, restore gamma oscillations, and improve working memory [167, 168]. Importantly, brain-penetrant GluN2A-selective NMDA receptor positive allosteric modulators have just been discovered [241]. Treatment with a GluN2A-selective positive allosteric modulator reduced the duration of loss of righting reflex induced by ketamine in rats [242]. Since the dose of ketamine chosen by the Dugan

Laboratory to inject into mice to injure PV-INs was informed by the duration of loss of righting reflex, a treatment that is able to decrease loss of righting reflex might also protect PV-INs from injury and/or rescue injured PV-INs [9]. If brain-penetrant Ca^{2+}-permeable AMPA receptor-selective positive allosteric modulators are discovered, these positive allosteric modulators also should somewhat selectively target PV-INs and therefore might have therapeutic potential as well. Much more work should be done exploring how best to prevent or treat injury to PV-INs, as protecting PV-INs could be one small but important step towards providing hope to those living with the burden of a neurodegenerative or psychiatric disease.

References

1. Rajan, K.B., et al., *Population estimate of people with clinical Alzheimer's disease and mild cognitive impairment in the United States (2020-2060).* Alzheimers Dement, 2021. **17**(12): p. 1966-1975.
2. Guerreiro, R. and J. Bras, *The age factor in Alzheimer's disease.* Genome Med, 2015. **7**: p. 106.
3. Hou, Y., et al., *Ageing as a risk factor for neurodegenerative disease.* Nat Rev Neurol, 2019. **15**(10): p. 565-581.
4. Stepnicki, P., M. Kondej, and A.A. Kaczor, *Current Concepts and Treatments of Schizophrenia.* Molecules, 2018. **23**(8).
5. Hu, H., J. Gan, and P. Jonas, *Interneurons. Fast-spiking, parvalbumin(+) GABAergic interneurons: from cellular design to microcircuit function.* Science, 2014. **345**(6196): p. 1255263.
6. Ruden, J.B., L.L. Dugan, and C. Konradi, *Parvalbumin interneuron vulnerability and brain disorders.* Neuropsychopharmacology, 2021. **46**(2): p. 279-287.
7. Kim, T., et al., *Cortically projecting basal forebrain parvalbumin neurons regulate cortical gamma band oscillations.* Proc Natl Acad Sci U S A, 2015. **112**(11): p. 3535-40.
8. Kajita, Y. and H. Mushiake, *Heterogeneous GAD65 Expression in Subtypes of GABAergic Neurons Across Layers of the Cerebral Cortex and Hippocampus.* Front Behav Neurosci, 2021. **15**: p. 750869.
9. Behrens, M.M., et al., *Ketamine-induced loss of phenotype of fast-spiking interneurons is mediated by NADPH-oxidase.* Science, 2007. **318**(5856): p. 1645-7.
10. Konradi, C., et al., *Hippocampal interneurons are abnormal in schizophrenia.* Schizophr Res, 2011. **131**(1-3): p. 165-73.
11. Lewis, D.A., et al., *Cortical parvalbumin interneurons and cognitive dysfunction in schizophrenia.* Trends Neurosci, 2012. **35**(1): p. 57-67.
12. Marin, O., *Interneuron dysfunction in psychiatric disorders.* Nat Rev Neurosci, 2012. **13**(2): p. 107-20.
13. Gonzalez-Burgos, G., R.Y. Cho, and D.A. Lewis, *Alterations in cortical network oscillations and parvalbumin neurons in schizophrenia.* Biol Psychiatry, 2015. **77**(12): p. 1031-40.
14. Filice, F., et al., *Reduction in parvalbumin expression not loss of the parvalbumin-expressing GABA interneuron subpopulation in genetic parvalbumin and shank mouse models of autism.* Mol Brain, 2016. **9**: p. 10.
15. Baig, S., G.K. Wilcock, and S. Love, *Loss of perineuronal net N-acetylgalactosamine in Alzheimer's disease.* Acta Neuropathol, 2005. **110**(4): p. 393-401.
16. Saiz-Sanchez, D., et al., *Interneurons, tau and amyloid-beta in the piriform cortex in Alzheimer's disease.* Brain Struct Funct, 2015. **220**(4): p. 2011-25.
17. Koh, D.X. and J.C. Sng, *HDAC1 negatively regulates Bdnf and Pvalb required for parvalbumin interneuron maturation in an experience-dependent manner.* J Neurochem, 2016. **139**(3): p. 369-380.
18. Wang, L., et al., *Aberration in epigenetic gene regulation in hippocampal neurogenesis by developmental exposure to manganese chloride in mice.* Toxicol Sci, 2013. **136**(1): p. 154-65.

19. Fachim, H.A., et al., *Parvalbumin promoter hypermethylation in postmortem brain in schizophrenia.* Epigenomics, 2018. **10**(5): p. 519-524.
20. Fachim, H.A., et al., *Subchronic administration of phencyclidine produces hypermethylation in the parvalbumin gene promoter in rat brain.* Epigenomics, 2016. **8**(9): p. 1179-83.
21. Veerasakul, S., et al., *Increased DNA methylation in the parvalbumin gene promoter is associated with methamphetamine dependence.* Pharmacogenomics, 2017. **18**(14): p. 1317-1322.
22. Lajtha, A. and N. Banik, *Handbook of Neurochemistry and Molecular Neurobiology Neural Protein Metabolism and Function*, in *Springer reference*. p. 1 online resource (XII, 698 p. 40 illus. eReference.).
23. Chard, P.S., et al., *Calcium buffering properties of calbindin D28k and parvalbumin in rat sensory neurones.* J Physiol, 1993. **472**: p. 341-57.
24. Yuan, L., et al., *Intermittent Hypoxia-Induced Parvalbumin-Immunoreactive Interneurons Loss and Neurobehavioral Impairment is Mediated by NADPH-Oxidase-2.* Neurochem Res, 2015. **40**(6): p. 1232-42.
25. Mao, M., et al., *The dysfunction of parvalbumin interneurons mediated by microglia contributes to cognitive impairment induced by lipopolysaccharide challenge.* Neurosci Lett, 2021. **762**: p. 136133.
26. Carlen, M., et al., *A critical role for NMDA receptors in parvalbumin interneurons for gamma rhythm induction and behavior.* Mol Psychiatry, 2012. **17**(5): p. 537-48.
27. Port, R.G., et al., *Parvalbumin Cell Ablation of NMDA-R1 Leads to Altered Phase, But Not Amplitude, of Gamma-Band Cross-Frequency Coupling.* Brain Connect, 2019. **9**(3): p. 263-272.
28. Saunders, J.A., et al., *Knockout of NMDA receptors in parvalbumin interneurons recreates autism-like phenotypes.* Autism Res, 2013. **6**(2): p. 69-77.
29. Kinney, J.W., et al., *A specific role for NR2A-containing NMDA receptors in the maintenance of parvalbumin and GAD67 immunoreactivity in cultured interneurons.* J Neurosci, 2006. **26**(5): p. 1604-15.
30. Lisman, J.E., et al., *Circuit-based framework for understanding neurotransmitter and risk gene interactions in schizophrenia.* Trends Neurosci, 2008. **31**(5): p. 234-42.
31. Warming, H., et al., *A primate-specific short GluN2A-NMDA receptor isoform is expressed in the human brain.* Mol Brain, 2019. **12**(1): p. 64.
32. Cardis, R., et al., *A lack of GluN2A-containing NMDA receptors confers a vulnerability to redox dysregulation: Consequences on parvalbumin interneurons, and their perineuronal nets.* Neurobiol Dis, 2018. **109**(Pt A): p. 64-75.
33. Lu, Y., et al., *Ketamine inhibits LPS-mediated BV2 microglial inflammation via NMDA receptor blockage.* Fundam Clin Pharmacol, 2020. **34**(2): p. 229-237.
34. Hao, Y., R. Xiong, and X. Gong, *Memantine, NMDA Receptor Antagonist, Attenuates ox-LDL-Induced Inflammation and Oxidative Stress via Activation of BDNF/TrkB Signaling Pathway in HUVECs.* Inflammation, 2021. **44**(2): p. 659-670.
35. Todd, L., et al., *Reactive microglia and IL1beta/IL-1R1-signaling mediate neuroprotection in excitotoxin-damaged mouse retina.* J Neuroinflammation, 2019. **16**(1): p. 118.
36. von Engelhardt, J., et al., *Excitotoxicity in vitro by NR2A- and NR2B-containing NMDA receptors.* Neuropharmacology, 2007. **53**(1): p. 10-7.
37. Saliba, S.W., et al., *Neuroprotective Effect of AM404 Against NMDA-Induced Hippocampal Excitotoxicity.* Front Cell Neurosci, 2019. **13**: p. 566.

38. Mukherjee, A., et al., *Long-lasting rescue of network and cognitive dysfunction in a genetic schizophrenia model.* Cell, 2019. **178**(6): p. 1387-1402 e14.
39. Lodge, D.J., M.M. Behrens, and A.A. Grace, *A loss of parvalbumin-containing interneurons is associated with diminished oscillatory activity in an animal model of schizophrenia.* J Neurosci, 2009. **29**(8): p. 2344-54.
40. Gill, K.M. and A.A. Grace, *Corresponding decrease in neuronal markers signals progressive parvalbumin neuron loss in MAM schizophrenia model.* Int J Neuropsychopharmacol, 2014. **17**(10): p. 1609-19.
41. Koh, M.T., et al., *Impaired hippocampal-dependent memory and reduced parvalbumin-positive interneurons in a ketamine mouse model of schizophrenia.* Schizophr Res, 2016. **171**(1-3): p. 187-94.
42. Wang, A.Y., et al., *Bipolar disorder type 1 and schizophrenia are accompanied by decreased density of parvalbumin- and somatostatin-positive interneurons in the parahippocampal region.* Acta Neuropathol, 2011. **122**(5): p. 615-26.
43. Enwright, J.F., et al., *Reduced labeling of parvalbumin neurons and perineuronal nets in the dorsolateral prefrontal cortex of subjects with schizophrenia.* Neuropsychopharmacology, 2016. **41**(9): p. 2206-14.
44. Cabungcal, J.H., et al., *Glutathione deficit during development induces anomalies in the rat anterior cingulate GABAergic neurons: Relevance to schizophrenia.* Neurobiol Dis, 2006. **22**(3): p. 624-37.
45. Chung, D.W., et al., *Dysregulated ErbB4 splicing in schizophrenia: selective effects on parvalbumin expression.* Am J Psychiatry, 2016. **173**(1): p. 60-8.
46. Volk, D.W., et al., *Deficits in transcriptional regulators of cortical parvalbumin neurons in schizophrenia.* Am J Psychiatry, 2012. **169**(10): p. 1082-91.
47. Chung, D.W., K.N. Fish, and D.A. Lewis, *Pathological basis for deficient excitatory drive to cortical parvalbumin interneurons in schizophrenia.* Am J Psychiatry, 2016. **173**(11): p. 1131-1139.
48. Bitanihirwe, B.K., et al., *Glutamatergic deficits and parvalbumin-containing inhibitory neurons in the prefrontal cortex in schizophrenia.* BMC Psychiatry, 2009. **9**: p. 71.
49. Barr, M.S., et al., *Evidence for excessive frontal evoked gamma oscillatory activity in schizophrenia during working memory.* Schizophr Res, 2010. **121**(1-3): p. 146-52.
50. Harrington, A.J., et al., *MEF2C regulates cortical inhibitory and excitatory synapses and behaviors relevant to neurodevelopmental disorders.* Elife, 2016. **5**.
51. Du, Y. and A.A. Grace, *Loss of parvalbumin in the hippocampus of MAM schizophrenia model rats is attenuated by peripubertal diazepam.* Int J Neuropsychopharmacol, 2016. **19**(11).
52. Powell, S.B., T.J. Sejnowski, and M.M. Behrens, *Behavioral and neurochemical consequences of cortical oxidative stress on parvalbumin-interneuron maturation in rodent models of schizophrenia.* Neuropharmacology, 2012. **62**(3): p. 1322-31.
53. Iaccarino, H.F., et al., *Gamma frequency entrainment attenuates amyloid load and modifies microglia.* Nature, 2016. **540**(7632): p. 230-235.
54. Rubio, S.E., et al., *Accelerated aging of the GABAergic septohippocampal pathway and decreased hippocampal rhythms in a mouse model of Alzheimer's disease.* FASEB J, 2012. **26**(11): p. 4458-67.
55. Ahnaou, A., et al., *Emergence of early alterations in network oscillations and functional connectivity in a tau seeding mouse model of Alzheimer's disease pathology.* Sci Rep, 2017. **7**(1): p. 14189.
56. Ogiwara, I., et al., *Nav1.1 localizes to axons of parvalbumin-positive inhibitory*

interneurons: a circuit basis for epileptic seizures in mice carrying an Scn1a gene mutation. J Neurosci, 2007. **27**(22): p. 5903-14.
57. Wang, W., et al., *The developmental changes of Na(v)1.1 and Na(v)1.2 expression in the human hippocampus and temporal lobe.* Brain Res, 2011. **1389**: p. 61-70.
58. Verret, L., et al., *Inhibitory interneuron deficit links altered network activity and cognitive dysfunction in Alzheimer model.* Cell, 2012. **149**(3): p. 708-21.
59. Mahar, I., et al., *Phenotypic alterations in hippocampal NPY- and PV-expressing interneurons in a presymptomatic transgenic mouse model of Alzheimer's disease.* Front Aging Neurosci, 2016. **8**: p. 327.
60. Verdaguer, E., et al., *Vulnerability of calbindin, calretinin and parvalbumin in a transgenic/knock-in APPswe/PS1dE9 mouse model of Alzheimer disease together with disruption of hippocampal neurogenesis.* Exp Gerontol, 2015. **69**: p. 176-88.
61. Nair, J., et al., *Basal forebrain contributes to default mode network regulation.* Proc Natl Acad Sci U S A, 2018. **115**(6): p. 1352-1357.
62. Jones, D.T., et al., *Age-related changes in the default mode network are more advanced in Alzheimer disease.* Neurology, 2011. **77**(16): p. 1524-31.
63. Zhang, H.Y., et al., *Resting brain connectivity: changes during the progress of Alzheimer disease.* Radiology, 2010. **256**(2): p. 598-606.
64. Zhou, J., et al., *Divergent network connectivity changes in behavioural variant frontotemporal dementia and Alzheimer's disease.* Brain, 2010. **133**(Pt 5): p. 1352-67.
65. Cha, J., et al., *Functional alteration patterns of default mode networks: comparisons of normal aging, amnestic mild cognitive impairment and Alzheimer's disease.* Eur J Neurosci, 2013. **37**(12): p. 1916-24.
66. Greicius, M.D., et al., *Default-mode network activity distinguishes Alzheimer's disease from healthy aging: evidence from functional MRI.* Proc Natl Acad Sci U S A, 2004. **101**(13): p. 4637-42.
67. Takahashi, H., et al., *Hippocampal interneuron loss in an APP/PS1 double mutant mouse and in Alzheimer's disease.* Brain Struct Funct, 2010. **214**(2-3): p. 145-60.
68. Albuquerque, M.S., et al., *Regional and sub-regional differences in hippocampal GABAergic neuronal vulnerability in the TgCRND8 mouse model of Alzheimer's disease.* Front Aging Neurosci, 2015. **7**: p. 30.
69. De Crescenzo, F., et al., *Autistic symptoms in schizophrenia spectrum disorders: a systematic review and meta-analysis.* Front Psychiatry, 2019. **10**: p. 78.
70. Hamm, J.P., et al., *Altered cortical ensembles in mouse models of schizophrenia.* Neuron, 2017. **94**(1): p. 153-167 e8.
71. Piskorowski, R.A., et al., *Age-dependent specific changes in area CA2 of the hippocampus and social memory deficit in a mouse model of the 22q11.2 deletion syndrome.* Neuron, 2016. **89**(1): p. 163-76.
72. Murphy, K.C., L.A. Jones, and M.J. Owen, *High rates of schizophrenia in adults with velo-cardio-facial syndrome.* Arch Gen Psychiatry, 1999. **56**(10): p. 940-5.
73. Stark, K.L., et al., *Altered brain microRNA biogenesis contributes to phenotypic deficits in a 22q11-deletion mouse model.* Nat Genet, 2008. **40**(6): p. 751-60.
74. Penagarikano, O., et al., *Absence of CNTNAP2 leads to epilepsy, neuronal migration abnormalities, and core autism-related deficits.* Cell, 2011. **147**(1): p. 235-46.
75. Lauber, E., F. Filice, and B. Schwaller, *Dysregulation of parvalbumin expression in the Cntnap2-/- mouse model of autism spectrum disorder.* Front Mol Neurosci, 2018. **11**: p. 262.
76. Selimbeyoglu, A., et al., *Modulation of prefrontal cortex excitation/inhibition balance*

rescues social behavior in CNTNAP2-deficient mice. Sci Transl Med, 2017. **9**(401).
77. Chen, L.Y., et al., *Conditional deletion of all neurexins defines diversity of essential synaptic organizer functions for neurexins.* Neuron, 2017. **94**(3): p. 611-625 e4.
78. Mao, W., et al., *Shank1 regulates excitatory synaptic transmission in mouse hippocampal parvalbumin-expressing inhibitory interneurons.* Eur J Neurosci, 2015. **41**(8): p. 1025-35.
79. Berkel, S., et al., *Mutations in the SHANK2 synaptic scaffolding gene in autism spectrum disorder and mental retardation.* Nat Genet, 2010. **42**(6): p. 489-91.
80. Shcheglovitov, A., et al., *SHANK3 and IGF1 restore synaptic deficits in neurons from 22q13 deletion syndrome patients.* Nature, 2013. **503**(7475): p. 267-71.
81. Nguyen, P.T., et al., *Cognitive and socio-emotional deficits in platelet-derived growth factor receptor-beta gene knockout mice.* PLoS One, 2011. **6**(3): p. e18004.
82. Nakamura, T., et al., *Relationships among parvalbumin-immunoreactive neuron density, phase-locked gamma oscillations, and autistic/schizophrenic symptoms in PDGFR-beta knock-out and control mice.* PLoS One, 2015. **10**(3): p. e0119258.
83. Wohr, M., et al., *Lack of parvalbumin in mice leads to behavioral deficits relevant to all human autism core symptoms and related neural morphofunctional abnormalities.* Transl Psychiatry, 2015. **5**: p. e525.
84. Chao, H.T., et al., *Dysfunction in GABA signalling mediates autism-like stereotypies and Rett syndrome phenotypes.* Nature, 2010. **468**(7321): p. 263-9.
85. Consortium, C.-D.G.o.t.P.G., et al., *Genetic relationship between five psychiatric disorders estimated from genome-wide SNPs.* Nat Genet, 2013. **45**(9): p. 984-94.
86. Cardno, A.G., et al., *A twin study of genetic relationships between psychotic symptoms.* Am J Psychiatry, 2002. **159**(4): p. 539-45.
87. Lee, F.H., et al., *Abnormal interneuron development in disrupted-in-schizophrenia-1 L100P mutant mice.* Mol Brain, 2013. **6**: p. 20.
88. Clapcote, S.J., et al., *Behavioral phenotypes of Disc1 missense mutations in mice.* Neuron, 2007. **54**(3): p. 387-402.
89. Delevich, K., et al., *Parvalbumin interneuron dysfunction in a thalamo-prefrontal cortical circuit in disc1 locus impairment mice.* eNeuro, 2020. **7**(2).
90. Jaaro-Peled, H., et al., *The cortico-striatal circuit regulates sensorimotor gating via Disc1/Huntingtin-mediated Bdnf transport.* BioRx, 2018. **non-peer reviewed preprint**.
91. Shen, S., et al., *Schizophrenia-related neural and behavioral phenotypes in transgenic mice expressing truncated Disc1.* J Neurosci, 2008. **28**(43): p. 10893-904.
92. Jones, N.C., et al., *Brain-derived neurotrophic factor haploinsufficiency impairs high-frequency cortical oscillations in mice.* Eur J Neurosci, 2018. **48**(8): p. 2816-2825.
93. Sloviter, R.S., et al., *Calcium-binding protein (calbindin-D28K) and parvalbumin immunocytochemistry in the normal and epileptic human hippocampus.* J Comp Neurol, 1991. **308**(3): p. 381-96.
94. Garbelli, R., et al., *Architectural (Type IA) focal cortical dysplasia and parvalbumin immunostaining in temporal lobe epilepsy.* Epilepsia, 2006. **47**(6): p. 1074-8.
95. Guentchev, M., et al., *Distribution of parvalbumin-immunoreactive neurons in brain correlates with hippocampal and temporal cortical pathology in Creutzfeldt-Jakob disease.* J Neuropathol Exp Neurol, 1997. **56**(10): p. 1119-24.
96. Caillard, O., et al., *Role of the calcium-binding protein parvalbumin in short-term synaptic plasticity.* Proc Natl Acad Sci U S A, 2000. **97**(24): p. 13372-7.
97. Wahr, P.A., D.E. Michele, and J.M. Metzger, *Parvalbumin gene transfer corrects diastolic dysfunction in diseased cardiac myocytes.* Proc Natl Acad Sci U S A, 1999.

96(21): p. 11982-5.
98. Galarreta, M. and S. Hestrin, *Electrical and chemical synapses among parvalbumin fast-spiking GABAergic interneurons in adult mouse neocortex.* Proc Natl Acad Sci U S A, 2002. **99**(19): p. 12438-43.
99. Donato, F., S.B. Rompani, and P. Caroni, *Parvalbumin-expressing basket-cell network plasticity induced by experience regulates adult learning.* Nature, 2013. **504**(7479): p. 272-6.
100. Yazaki-Sugiyama, Y., et al., *Bidirectional plasticity in fast-spiking GABA circuits by visual experience.* Nature, 2009. **462**(7270): p. 218-21.
101. Kuhlman, S.J., et al., *A disinhibitory microcircuit initiates critical-period plasticity in the visual cortex.* Nature, 2013. **501**(7468): p. 543-6.
102. Kaplan, E.S., et al., *Contrasting roles for parvalbumin-expressing inhibitory neurons in two forms of adult visual cortical plasticity.* Elife, 2016. **5**.
103. Packer, A.M. and R. Yuste, *Dense, unspecific connectivity of neocortical parvalbumin-positive interneurons: a canonical microcircuit for inhibition?* J Neurosci, 2011. **31**(37): p. 13260-71.
104. Buzsaki, G. and X.J. Wang, *Mechanisms of gamma oscillations.* Annu Rev Neurosci, 2012. **35**: p. 203-25.
105. Cardin, J.A., et al., *Driving fast-spiking cells induces gamma rhythm and controls sensory responses.* Nature, 2009. **459**(7247): p. 663-7.
106. Sohal, V.S., et al., *Parvalbumin neurons and gamma rhythms enhance cortical circuit performance.* Nature, 2009. **459**(7247): p. 698-702.
107. Volman, V., M.M. Behrens, and T.J. Sejnowski, *Downregulation of parvalbumin at cortical GABA synapses reduces network gamma oscillatory activity.* J Neurosci, 2011. **31**(49): p. 18137-48.
108. Howard, M.W., et al., *Gamma oscillations correlate with working memory load in humans.* Cereb Cortex, 2003. **13**(12): p. 1369-74.
109. Gulyas, A.I., et al., *Total number and ratio of excitatory and inhibitory synapses converging onto single interneurons of different types in the CA1 area of the rat hippocampus.* J Neurosci, 1999. **19**(22): p. 10082-97.
110. Kann, O., I.E. Papageorgiou, and A. Draguhn, *Highly energized inhibitory interneurons are a central element for information processing in cortical networks.* J Cereb Blood Flow Metab, 2014. **34**(8): p. 1270-82.
111. Inan, M., et al., *Energy deficit in parvalbumin neurons leads to circuit dysfunction, impaired sensory gating and social disability.* Neurobiol Dis, 2016. **93**: p. 35-46.
112. Kann, O., et al., *Gamma oscillations in the hippocampus require high complex I gene expression and strong functional performance of mitochondria.* Brain, 2011. **134**(Pt 2): p. 345-58.
113. Huchzermeyer, C., et al., *Oxygen consumption rates during three different neuronal activity states in the hippocampal CA3 network.* J Cereb Blood Flow Metab, 2013. **33**(2): p. 263-71.
114. Gulyas, A.I., et al., *Populations of hippocampal inhibitory neurons express different levels of cytochrome c.* Eur J Neurosci, 2006. **23**(10): p. 2581-94.
115. Liu, X., et al., *Induction of apoptotic program in cell-free extracts: requirement for dATP and cytochrome c.* Cell, 1996. **86**(1): p. 147-57.
116. Kisvarday, Z.F., C. Beaulieu, and U.T. Eysel, *Network of GABAergic large basket cells in cat visual cortex (area 18): implication for lateral disinhibition.* J Comp Neurol, 1993. **327**(3): p. 398-415.

117. Sik, A., et al., *Hippocampal CA1 interneurons: an in vivo intracellular labeling study.* J Neurosci, 1995. **15**(10): p. 6651-65.
118. Buhl, E.H., K. Halasy, and P. Somogyi, *Diverse sources of hippocampal unitary inhibitory postsynaptic potentials and the number of synaptic release sites.* Nature, 1994. **368**(6474): p. 823-8.
119. Tremblay, R., S. Lee, and B. Rudy, *GABAergic interneurons in the neocortex: from cellular properties to circuits.* Neuron, 2016. **91**(2): p. 260-92.
120. Whittaker, R.G., et al., *Impaired mitochondrial function abolishes gamma oscillations in the hippocampus through an effect on fast-spiking interneurons.* Brain, 2011. **134**(Pt 7): p. e180; author reply e181.
121. Steullet, P., et al., *Oxidative stress-driven parvalbumin interneuron impairment as a common mechanism in models of schizophrenia.* Mol Psychiatry, 2017.
122. Steullet, P., et al., *Redox dysregulation affects the ventral but not dorsal hippocampus: impairment of parvalbumin neurons, gamma oscillations, and related behaviors.* J Neurosci, 2010. **30**(7): p. 2547-58.
123. Behrens, M.M., S.S. Ali, and L.L. Dugan, *Interleukin-6 mediates the increase in NADPH-oxidase in the ketamine model of schizophrenia.* J Neurosci, 2008. **28**(51): p. 13957-66.
124. Dugan, L.L., et al., *IL-6 mediated degeneration of forebrain GABAergic interneurons and cognitive impairment in aged mice through activation of neuronal NADPH oxidase.* PLoS One, 2009. **4**(5): p. e5518.
125. Gough, D.J., et al., *Mitochondrial STAT3 supports Ras-dependent oncogenic transformation.* Science, 2009. **324**(5935): p. 1713-6.
126. Wegrzyn, J., et al., *Function of mitochondrial Stat3 in cellular respiration.* Science, 2009. **323**(5915): p. 793-7.
127. Kim, Y.M., et al., *ROS-induced ROS release orchestrated by Nox4, Nox2, and mitochondria in VEGF signaling and angiogenesis.* Am J Physiol Cell Physiol, 2017. **312**(6): p. C749-C764.
128. Joseph, L.C., et al., *Inhibition of NAPDH oxidase 2 (NOX2) prevents oxidative stress and mitochondrial abnormalities caused by saturated fat in cardiomyocytes.* PLoS One, 2016. **11**(1): p. e0145750.
129. Dikalov, S.I., et al., *Nox2-induced production of mitochondrial superoxide in angiotensin II-mediated endothelial oxidative stress and hypertension.* Antioxid Redox Signal, 2014. **20**(2): p. 281-94.
130. Lu, J., et al., *Input-specific maturation of synaptic dynamics of parvalbumin interneurons in primary visual cortex.* Proc Natl Acad Sci U S A, 2014. **111**(47): p. 16895-900.
131. Fuchs, E.C., et al., *Recruitment of parvalbumin-positive interneurons determines hippocampal function and associated behavior.* Neuron, 2007. **53**(4): p. 591-604.
132. Timofeeva, O.A. and E.D. Levin, *Glutamate and nicotinic receptor interactions in working memory: importance for the cognitive impairment of schizophrenia.* Neuroscience, 2011. **195**: p. 21-36.
133. Goldberg, J.H., R. Yuste, and G. Tamas, *Ca^{2+} imaging of mouse neocortical interneurone dendrites: contribution of Ca^{2+}-permeable AMPA and NMDA receptors to subthreshold Ca^{2+}dynamics.* J Physiol, 2003. **551**(Pt 1): p. 67-78.
134. Szabo, A., et al., *Calcium-permeable AMPA receptors provide a common mechanism for LTP in glutamatergic synapses of distinct hippocampal interneuron types.* J Neurosci, 2012. **32**(19): p. 6511-6.

135. Nissen, W., et al., *Cell type-specific long-term plasticity at glutamatergic synapses onto hippocampal interneurons expressing either parvalbumin or CB1 cannabinoid receptor.* J Neurosci, 2010. **30**(4): p. 1337-47.
136. Contreras, L., et al., *Mitochondria: the calcium connection.* Biochim Biophys Acta, 2010. **1797**(6-7): p. 607-18.
137. Kwak, S. and J.H. Weiss, *Calcium-permeable AMPA channels in neurodegenerative disease and ischemia.* Curr Opin Neurobiol, 2006. **16**(3): p. 281-7.
138. Hong, S.J., T.M. Dawson, and V.L. Dawson, *Nuclear and mitochondrial conversations in cell death: PARP-1 and AIF signaling.* Trends Pharmacol Sci, 2004. **25**(5): p. 259-64.
139. Yin, H.Z., et al., *Blockade of Ca^{2+}-permeable AMPA/kainate channels decreases oxygen-glucose deprivation-induced Zn^{2+} accumulation and neuronal loss in hippocampal pyramidal neurons.* J Neurosci, 2002. **22**(4): p. 1273-9.
140. Sensi, S.L., et al., *Preferential Zn^{2+} influx through Ca^{2+}-permeable AMPA/kainate channels triggers prolonged mitochondrial superoxide production.* Proc Natl Acad Sci U S A, 1999. **96**(5): p. 2414-9.
141. Jia, Y., et al., *Zn^{2+} currents are mediated by calcium-permeable AMPA/kainate channels in cultured murine hippocampal neurones.* J Physiol, 2002. **543**(Pt 1): p. 35-48.
142. Kim, Y.H. and J.Y. Koh, *The role of NADPH oxidase and neuronal nitric oxide synthase in zinc-induced poly(ADP-ribose) polymerase activation and cell death in cortical culture.* Exp Neurol, 2002. **177**(2): p. 407-18.
143. Jiang, D., et al., *Zn(2+) induces permeability transition pore opening and release of pro-apoptotic peptides from neuronal mitochondria.* J Biol Chem, 2001. **276**(50): p. 47524-9.
144. Cueva Vargas, J.L., et al., *Soluble tumor necrosis factor alpha promotes retinal ganglion cell death in glaucoma via calcium-permeable AMPA receptor activation.* J Neurosci, 2015. **35**(35): p. 12088-102.
145. Spaethling, J.M., et al., *Calcium-permeable AMPA receptors appear in cortical neurons after traumatic mechanical injury and contribute to neuronal fate.* J Neurotrauma, 2008. **25**(10): p. 1207-16.
146. Huntley, G.W., J.C. Vickers, and J.H. Morrison, *Quantitative localization of NMDAR1 receptor subunit immunoreactivity in inferotemporal and prefrontal association cortices of monkey and human.* Brain Res, 1997. **749**(2): p. 245-62.
147. Huntley, G.W., et al., *Distribution and synaptic localization of immunocytochemically identified NMDA receptor subunit proteins in sensory-motor and visual cortices of monkey and human.* J Neurosci, 1994. **14**(6): p. 3603-19.
148. Konradi, C. and S. Heckers, *Molecular aspects of glutamate dysregulation: implications for schizophrenia and its treatment.* Pharmacol Ther, 2003. **97**(2): p. 153-79.
149. McQuail, J.A., et al., *NR2A-containing NMDARs in the prefrontal cortex are required for working memory and associated with age-related cognitive decline.* J Neurosci, 2016. **36**(50): p. 12537-12548.
150. Kocsis, B., *Differential role of NR2A and NR2B subunits in N-methyl-D-aspartate receptor antagonist-induced aberrant cortical gamma oscillations.* Biol Psychiatry, 2012. **71**(11): p. 987-95.
151. Wonders, C.P. and S.A. Anderson, *The origin and specification of cortical interneurons.* Nat Rev Neurosci, 2006. **7**(9): p. 687-96.

152. Bandler, R.C., C. Mayer, and G. Fishell, *Cortical interneuron specification: the juncture of genes, time and geometry.* Curr Opin Neurobiol, 2017. **42**: p. 17-24.
153. Hu, J.S., et al., *Cortical interneuron development: a tale of time and space.* Development, 2017. **144**(21): p. 3867-3878.
154. Lim, L., et al., *Development and functional diversification of cortical interneurons.* Neuron, 2018. **100**(2): p. 294-313.
155. Guo, J. and E.S. Anton, *Decision making during interneuron migration in the developing cerebral cortex.* Trends Cell Biol, 2014. **24**(6): p. 342-51.
156. Marin, O., et al., *Guiding neuronal cell migrations.* Cold Spring Harb Perspect Biol, 2010. **2**(2): p. a001834.
157. Peyre, E., C.G. Silva, and L. Nguyen, *Crosstalk between intracellular and extracellular signals regulating interneuron production, migration and integration into the cortex.* Front Cell Neurosci, 2015. **9**: p. 129.
158. Rymar, V.V. and A.F. Sadikot, *Laminar fate of cortical GABAergic interneurons is dependent on both birthdate and phenotype.* J Comp Neurol, 2007. **501**(3): p. 369-80.
159. Sahara, S., et al., *The fraction of cortical GABAergic neurons is constant from near the start of cortical neurogenesis to adulthood.* J Neurosci, 2012. **32**(14): p. 4755-61.
160. Akbarian, S., et al., *Maldistribution of interstitial neurons in prefrontal white matter of the brains of schizophrenic patients.* Arch Gen Psychiatry, 1996. **53**(5): p. 425-36.
161. Akbarian, S., et al., *Distorted distribution of nicotinamide-adenine dinucleotide phosphate-diaphorase neurons in temporal lobe of schizophrenics implies anomalous cortical development.* Arch Gen Psychiatry, 1993. **50**(3): p. 178-87.
162. Akbarian, S., et al., *Altered distribution of nicotinamide-adenine dinucleotide phosphate-diaphorase cells in frontal lobe of schizophrenics implies disturbances of cortical development.* Arch Gen Psychiatry, 1993. **50**(3): p. 169-77.
163. Tricoire, L., et al., *A blueprint for the spatiotemporal origins of mouse hippocampal interneuron diversity.* J Neurosci, 2011. **31**(30): p. 10948-70.
164. Heckers, S. and C. Konradi, *GABAergic mechanisms of hippocampal hyperactivity in schizophrenia.* Schizophr Res, 2015. **167**(1-3): p. 4-11.
165. Konradi, C., et al., *Hippocampal interneurons in bipolar disorder.* Arch Gen Psychiatry, 2011. **68**(4): p. 340-50.
166. Heckers, S., et al., *Differential hippocampal expression of glutamic acid decarboxylase 65 and 67 messenger RNA in bipolar disorder and schizophrenia.* Arch Gen Psychiatry, 2002. **59**(6): p. 521-9.
167. Hackos, D.H., et al., *Positive allosteric modulators of GluN2A-containing NMDARs with distinct modes of action and impacts on circuit function.* Neuron, 2016. **89**(5): p. 983-99.
168. Volgraf, M., et al., *Discovery of GluN2A-selective NMDA receptor positive allosteric modulators (PAMs): tuning deactivation kinetics via structure-based design.* J Med Chem, 2016. **59**(6): p. 2760-79.
169. Kaiser, T., et al., *Transgenic labeling of parvalbumin-expressing neurons with tdTomato.* Neuroscience, 2016. **321**: p. 236-245.
170. Bhutta, B.S., F. Alghoula, and I. Berim, *Hypoxia*, in *StatPearls*. 2021: Treasure Island (FL).
171. Colgan, S.P., *Targeting hypoxia in inflammatory bowel disease.* J Investig Med, 2016. **64**(2): p. 364-8.
172. Nizet, V. and R.S. Johnson, *Interdependence of hypoxic and innate immune responses.* Nat Rev Immunol, 2009. **9**(9): p. 609-17.

173. Taylor, C.T. and S.P. Colgan, *Hypoxia and gastrointestinal disease.* J Mol Med (Berl), 2007. **85**(12): p. 1295-300.
174. Eltzschig, H.K. and P. Carmeliet, *Hypoxia and inflammation.* N Engl J Med, 2011. **364**(7): p. 656-65.
175. Marina, N., et al., *Astrocytes and Brain Hypoxia.* Adv Exp Med Biol, 2016. **903**: p. 201-7.
176. Socodato, R., et al., *Redox tuning of Ca(2+) signaling in microglia drives glutamate release during hypoxia.* Free Radic Biol Med, 2018. **118**: p. 137-149.
177. Butturini, E., et al., *STAT1 drives M1 microglia activation and neuroinflammation under hypoxia.* Arch Biochem Biophys, 2019. **669**: p. 22-30.
178. Kaur, C., G. Rathnasamy, and E.A. Ling, *Roles of activated microglia in hypoxia induced neuroinflammation in the developing brain and the retina.* J Neuroimmune Pharmacol, 2013. **8**(1): p. 66-78.
179. Fagel, D.M., et al., *Fgfr1 is required for cortical regeneration and repair after perinatal hypoxia.* J Neurosci, 2009. **29**(4): p. 1202-11.
180. Liang, D., et al., *Increased Seizure Susceptibility for Rats Subject to Early Life Hypoxia Might Be Associated with Brain Dysfunction of NRG1-ErbB4 Signaling in Parvalbumin Interneurons.* Mol Neurobiol, 2020. **57**(12): p. 5276-5285.
181. Zhang, M., et al., *Environmental Enrichment Prevent the Juvenile Hypoxia-Induced Developmental Loss of Parvalbumin-Immunoreactive Cells in the Prefrontal Cortex and Neurobehavioral Alterations Through Inhibition of NADPH Oxidase-2-Derived Oxidative Stress.* Mol Neurobiol, 2016. **53**(10): p. 7341-7350.
182. Liang, D., et al., *Developmental loss of parvalbumin-positive cells in the prefrontal cortex and psychiatric anxiety after intermittent hypoxia exposures in neonatal rats might be mediated by NADPH oxidase-2.* Behav Brain Res, 2016. **296**: p. 134-140.
183. Komitova, M., et al., *Hypoxia-induced developmental delays of inhibitory interneurons are reversed by environmental enrichment in the postnatal mouse forebrain.* J Neurosci, 2013. **33**(33): p. 13375-87.
184. Xu, K. and J.C. Lamanna, *Chronic hypoxia and the cerebral circulation.* J Appl Physiol (1985), 2006. **100**(2): p. 725-30.
185. Tsipis, C.P., et al., *Hypoxia-induced angiogenesis and capillary density determination.* Methods Mol Biol, 2014. **1135**: p. 69-80.
186. Alcayaga, J., et al., *Rabbit ventilatory responses to peripheral chemoexcitators: effects of chronic hypoxia.* Adv Exp Med Biol, 2012. **758**: p. 307-13.
187. Benderro, G.F. and J.C. Lamanna, *Hypoxia-induced angiogenesis is delayed in aging mouse brain.* Brain Res, 2011. **1389**: p. 50-60.
188. Xu, K., et al., *Gender differences in hypoxic acclimatization in cyclooxygenase-2-deficient mice.* Physiol Rep, 2017. **5**(4).
189. Baddeley, A., C. Jarrold, and F. Vargha-Khadem, *Working memory and the hippocampus.* J Cogn Neurosci, 2011. **23**(12): p. 3855-61.
190. Blatow, M., et al., *A novel network of multipolar bursting interneurons generates theta frequency oscillations in neocortex.* Neuron, 2003. **38**(5): p. 805-17.
191. Markram, H., et al., *Interneurons of the neocortical inhibitory system.* Nat Rev Neurosci, 2004. **5**(10): p. 793-807.
192. Tooley, J., et al., *Glutamatergic Ventral Pallidal Neurons Modulate Activity of the Habenula-Tegmental Circuitry and Constrain Reward Seeking.* Biol Psychiatry, 2018. **83**(12): p. 1012-1023.
193. Knowland, D., et al., *Distinct Ventral Pallidal Neural Populations Mediate Separate*

Symptoms of Depression. Cell, 2017. **170**(2): p. 284-297 e18.
194. Ostergaard, L., *SARS CoV-2 related microvascular damage and symptoms during and after COVID-19: Consequences of capillary transit-time changes, tissue hypoxia and inflammation.* Physiol Rep, 2021. **9**(3): p. e14726.
195. Simonson, T.S., et al., *Silent hypoxaemia in COVID-19 patients.* J Physiol, 2021. **599**(4): p. 1057-1065.
196. Chakraborty, A., S. Murphy, and N. Coleman, *The Role of NMDA Receptors in Neural Stem Cell Proliferation and Differentiation.* Stem Cells Dev, 2017. **26**(11): p. 798-807.
197. Hunt, D.L. and P.E. Castillo, *Synaptic plasticity of NMDA receptors: mechanisms and functional implications.* Curr Opin Neurobiol, 2012. **22**(3): p. 496-508.
198. Liu, Y., et al., *NMDA receptor subunits have differential roles in mediating excitotoxic neuronal death both in vitro and in vivo.* J Neurosci, 2007. **27**(11): p. 2846-57.
199. Luscher, C. and R.C. Malenka, *NMDA receptor-dependent long-term potentiation and long-term depression (LTP/LTD).* Cold Spring Harb Perspect Biol, 2012. **4**(6).
200. Paoletti, P., C. Bellone, and Q. Zhou, *NMDA receptor subunit diversity: impact on receptor properties, synaptic plasticity and disease.* Nat Rev Neurosci, 2013. **14**(6): p. 383-400.
201. Bayes, A., et al., *Comparative study of human and mouse postsynaptic proteomes finds high compositional conservation and abundance differences for key synaptic proteins.* PLoS One, 2012. **7**(10): p. e46683.
202. Ishii, M.N., et al., *Human induced pluripotent stem cell (hiPSC)-derived neurons respond to convulsant drugs when co-cultured with hiPSC-derived astrocytes.* Toxicology, 2017. **389**: p. 130-138.
203. Lieberman, R., et al., *Pilot study of iPS-derived neural cells to examine biologic effects of alcohol on human neurons in vitro.* Alcohol Clin Exp Res, 2012. **36**(10): p. 1678-87.
204. Pruunsild, P., C.P. Bengtson, and H. Bading, *Networks of Cultured iPSC-Derived Neurons Reveal the Human Synaptic Activity-Regulated Adaptive Gene Program.* Cell Rep, 2017. **18**(1): p. 122-135.
205. Zhang, W.B., et al., *Fyn Kinase regulates GluN2B subunit-dominant NMDA receptors in human induced pluripotent stem cell-derived neurons.* Sci Rep, 2016. **6**: p. 23837.
206. Lam, R.S., et al., *Functional Maturation of Human Stem Cell-Derived Neurons in Long-Term Cultures.* PLoS One, 2017. **12**(1): p. e0169506.
207. Yakoub, A.M. and M. Sadek, *Development and Characterization of Human Cerebral Organoids: An Optimized Protocol.* Cell Transplant, 2018. **27**(3): p. 393-406.
208. Yakoub, A.M. and M. Sadek, *Analysis of Synapses in Cerebral Organoids.* Cell Transplant, 2019. **28**(9-10): p. 1173-1182.
209. Gordon, A., et al., *Long-term maturation of human cortical organoids matches key early postnatal transitions.* Nat Neurosci, 2021. **24**(3): p. 331-342.
210. Zafeiriou, M.P., et al., *Developmental GABA polarity switch and neuronal plasticity in Bioengineered Neuronal Organoids.* Nat Commun, 2020. **11**(1): p. 3791.
211. Booij, T.H., L.S. Price, and E.H.J. Danen, *3D Cell-Based Assays for Drug Screens: Challenges in Imaging, Image Analysis, and High-Content Analysis.* SLAS Discov, 2019. **24**(6): p. 615-627.
212. Kassis, T., et al., *OrgaQuant: Human Intestinal Organoid Localization and Quantification Using Deep Convolutional Neural Networks.* Sci Rep, 2019. **9**(1): p. 12479.
213. Rios, A.C. and H. Clevers, *Imaging organoids: a bright future ahead.* Nat Methods, 2018. **15**(1): p. 24-26.

214. Xin, W.K., et al., *A functional interaction of sodium and calcium in the regulation of NMDA receptor activity by remote NMDA receptors.* J Neurosci, 2005. **25**(1): p. 139-48.
215. Lee, M.C., et al., *Characterisation of the expression of NMDA receptors in human astrocytes.* PLoS One, 2010. **5**(11): p. e14123.
216. Giffard, R.G., J.H. Weiss, and D.W. Choi, *Extracellular alkalinity exacerbates injury of cultured cortical neurons.* Stroke, 1992. **23**(12): p. 1817-21.
217. Kumar, K.K., et al., *Cellular manganese content is developmentally regulated in human dopaminergic neurons.* Sci Rep, 2014. **4**: p. 6801.
218. Bar-Shira, O., R. Maor, and G. Chechik, *Gene Expression Switching of Receptor Subunits in Human Brain Development.* PLoS Comput Biol, 2015. **11**(12): p. e1004559.
219. Haberny, K.A., et al., *Ontogeny of the N-methyl-D-aspartate (NMDA) receptor system and susceptibility to neurotoxicity.* Toxicol Sci, 2002. **68**(1): p. 9-17.
220. Watanabe, M., et al., *Developmental changes in distribution of NMDA receptor channel subunit mRNAs.* Neuroreport, 1992. **3**(12): p. 1138-40.
221. Hedegaard, M., et al., *Molecular pharmacology of human NMDA receptors.* Neurochem Int, 2012. **61**(4): p. 601-9.
222. Bell, S., et al., *Differentiation of Human Induced Pluripotent Stem Cells (iPSCs) into an Effective Model of Forebrain Neural Progenitor Cells and Mature Neurons.* Bio Protoc, 2019. **9**(5): p. e3188.
223. Muratore, C.R., et al., *Comparison and optimization of hiPSC forebrain cortical differentiation protocols.* PLoS One, 2014. **9**(8): p. e105807.
224. Zhang, M., et al., *Highly efficient methods to obtain homogeneous dorsal neural progenitor cells from human and mouse embryonic stem cells and induced pluripotent stem cells.* Stem Cell Res Ther, 2018. **9**(1): p. 67.
225. Farhy-Tselnicker, I. and N.J. Allen, *Astrocytes, neurons, synapses: a tripartite view on cortical circuit development.* Neural Dev, 2018. **13**(1): p. 7.
226. Chung, W.S., N.J. Allen, and C. Eroglu, *Astrocytes Control Synapse Formation, Function, and Elimination.* Cold Spring Harb Perspect Biol, 2015. **7**(9): p. a020370.
227. Touyz, R.M., et al., *NOX5: Molecular biology and pathophysiology.* Exp Physiol, 2019. **104**(5): p. 605-616.
228. Mertens, J., et al., *Evaluating cell reprogramming, differentiation and conversion technologies in neuroscience.* Nat Rev Neurosci, 2016. **17**(7): p. 424-37.
229. Santostefano, K.E., et al., *A practical guide to induced pluripotent stem cell research using patient samples.* Lab Invest, 2015. **95**(1): p. 4-13.
230. Hu, K., *All roads lead to induced pluripotent stem cells: the technologies of iPSC generation.* Stem Cells Dev, 2014. **23**(12): p. 1285-300.
231. Lowenthal, J., et al., *Specimen collection for induced pluripotent stem cell research: harmonizing the approach to informed consent.* Stem Cells Transl Med, 2012. **1**(5): p. 409-21.
232. Bickler, P.E., C.S. Fahlman, and D.M. Taylor, *Oxygen sensitivity of NMDA receptors: relationship to NR2 subunit composition and hypoxia tolerance of neonatal neurons.* Neuroscience, 2003. **118**(1): p. 25-35.
233. Zanelli, S.A., Q.M. Ashraf, and O.P. Mishra, *Nitration is a mechanism of regulation of the NMDA receptor function during hypoxia.* Neuroscience, 2002. **112**(4): p. 869-77.
234. Dumanska, H. and N. Veselovsky, *Short-term hypoxia induces bidirectional pathological long-term plasticity of neurotransmission in visual retinocollicular pathway.* Exp Eye Res, 2019. **179**: p. 25-31.

235. Arias-Cavieres, A., et al., *A HIF1a-Dependent Pro-Oxidant State Disrupts Synaptic Plasticity and Impairs Spatial Memory in Response to Intermittent Hypoxia*. eNeuro, 2020. **7**(3).
236. Perkins, D.O., C.D. Jeffries, and K.Q. Do, *Potential Roles of Redox Dysregulation in the Development of Schizophrenia.* Biol Psychiatry, 2020. **88**(4): p. 326-336.
237. Yacobi, A., Y. Stern Bach, and M. Horowitz, *The protective effect of heat acclimation from hypoxic damage in the brain involves changes in the expression of glutamate receptors.* Temperature (Austin), 2014. **1**(1): p. 57-65.
238. Mele, M., et al., *Application of the Co-culture Membrane System Pointed to a Protective Role of Catestatin on Hippocampal Plus Hypothalamic Neurons Exposed to Oxygen and Glucose Deprivation.* Mol Neurobiol, 2017. **54**(9): p. 7369-7381.
239. Huang, Q., et al., *Automated Neuron Tracing Using Content-Aware Adaptive Voxel Scooping on CNN Predicted Probability Map.* Front Neuroanat, 2021. **15**: p. 712842.
240. Shi, Z., et al., *Conversion of Fibroblasts to Parvalbumin Neurons by One Transcription Factor, Ascl1, and the Chemical Compound Forskolin.* J Biol Chem, 2016. **291**(26): p. 13560-70.
241. Sakurai, F., et al., *Discovery of Pyrazolo[1,5-a]pyrazin-4-ones as Potent and Brain Penetrant GluN2A-Selective Positive Allosteric Modulators Reducing AMPA Receptor Binding Activity.* Bioorg Med Chem, 2022. **56**: p. 116576.
242. Li, C., et al., *GluN2A-selective positive allosteric modulator-nalmefene-flumazenil reverses ketamine-fentanyl-dexmedetomidine-induced anesthesia and analgesia in rats.* Sci Rep, 2020. **10**(1): p. 5265.